

# Multiscale analysis in image processing

## Scale invariance in data processing

---

**Barbara Pascal**<sup>†</sup>

[bpascal-fr.github.io/talks](https://bpascal-fr.github.io/talks)

June 2026

<sup>†</sup> Nantes Université, École Centrale Nantes, CNRS, LS2N, F-44000 Nantes, France



# Self-similarity in signals and images

---

## Self-similar fields

$F : \mathbb{R}^d \rightarrow \mathbb{R}$  a random field is **self-similar** if there exists  $H \in (0, 1)$  s.t.

$$(\forall c > 0) \quad \{F(c\underline{x}); \underline{x} \in \mathbb{R}^d\} \stackrel{(d)}{=} c^H \{F(\underline{x}); \underline{x} \in \mathbb{R}^d\}$$

with  $\stackrel{(d)}{=}$  equality in distribution  $\implies H$ : **fractal** index

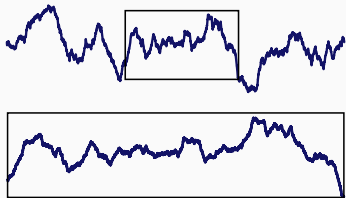
# Self-similar fields

$F : \mathbb{R}^d \rightarrow \mathbb{R}$  a random field is **self-similar** if there exists  $H \in (0, 1)$  s.t.

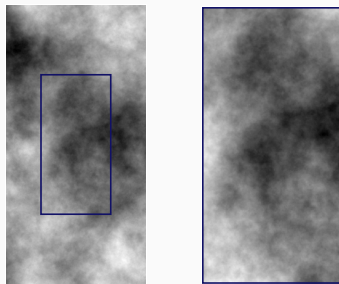
$$(\forall c > 0) \quad \{F(c\underline{x}); \underline{x} \in \mathbb{R}^N\} \stackrel{(d)}{=} c^H \{F(\underline{x}); \underline{x} \in \mathbb{R}^d\}$$

with  $\stackrel{(d)}{=}$  equality in distribution  $\implies H$ : **fractal index**

**Time series**  $\{F(t), t \in \mathbb{R}\}$



**Images**  $F : \Omega \subset \mathbb{R}^2 \rightarrow \mathbb{R}$



LES FRACTALES: OBJETS MATHÉMATIQUES,  
MODÈLES PHYSIQUES ET CRÉATIONS ARTISTIQUES

Benoît B. MANDELBROT

IBM Thomas J. Watson Research Center, Yorktown Heights, NY, 10598, USA

---

**RESUME**

La géométrie fractale de la nature fut conçue et développée par l'auteur de ce travail et présentée pour la

**SUMMARY**

The fractal geometry of nature was conceived and developed by the author, beginning in 1975. It started with

*“The fractal geometry of nature was conceived and developed by the author beginning in 1975. It started with two unexpected discoveries, and has had manifold effects. Fractals have contributed to give back to mathematics and to physics the visual and almost sensual aspects that had become almost completely foreign to them. Fractals also raise many new questions concerning aesthetics and many problems of computer graphics. My first discovery concerned the role of the so-called “mathematical monsters”, which are geometric constructions that arose around 1980 and threatened the philosophical framework of mathematics and physics. ”*

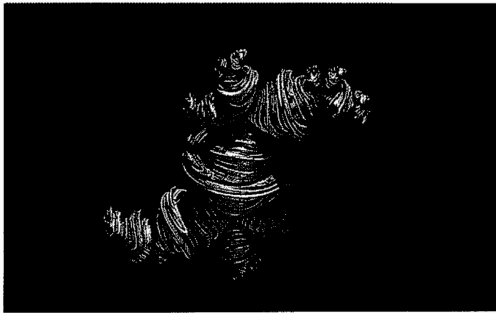


**Figure 4 Dragon fractal quaternionique**, réalisé par V. Alan Norton. Copyright 1983 by V. Alan Norton.

[B. B. Mandelbrot, 1983, "The fractal geometry of nature.", *W. H. Freeman and Co.*;

B. B. Mandelbrot, 1984, *Colloque Images*]

# Fractal objects in signal and image processing

- Physics: turbulent flows, geophysics [M. Nelkin, 1989, *J. Stat. Phys.*; B. Dubrulle, et al., 2022, *Philos. Trans. R. Soc. A.*]
- Financial forecasting [R.T. Baillie, 1996, *J. Econom.*]
- Geography: relief representation, population in cities [L. Lucido, et al., 1998, *Int. J. Syst. Sci.*; J. Lengyel et al., 2025, *Sci. Rep.*]
- Cardiac activity mother-fetus [M. Doret et al., 2015, *PloS One.*]
- Computer networks analysis, Internet traffic  
[J. Beran et al., 1995, *IEEE Trans. Commun.*;  
P. Abry, et al., 1998, *IEEE Trans. Inf. Theory*;  
R. Fontugne, et al., 2017, *IEEE/ACM Trans. Network.*]
- Infographics/computer graphics  
[J. L., Encarnação et al., 2012, *Springer Science & Business Media.*]

# Isotropic texture segmentation

---

## Intuition and examples of texture

**Texture:** periodically and/or stochastically repeated pattern.

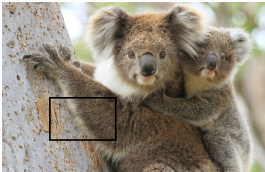
# Intuition and examples of texture

**Texture:** periodically and/or stochastically repeated pattern.



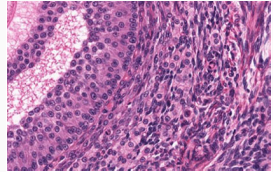
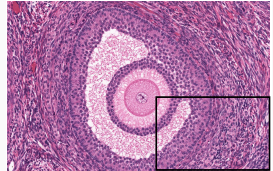
# Intuition and examples of texture

**Texture:** periodically and/or stochastically repeated pattern.



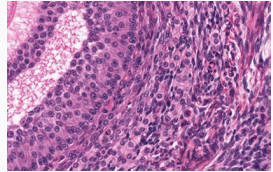
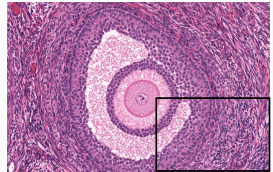
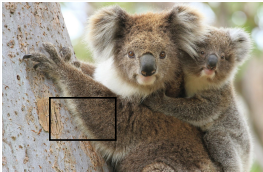
# Intuition and examples of texture

**Texture:** periodically and/or stochastically repeated pattern.



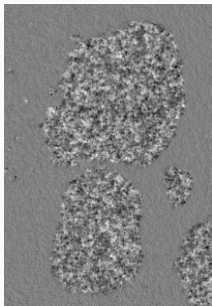
# Intuition and examples of texture

**Texture:** periodically and/or stochastically repeated pattern.

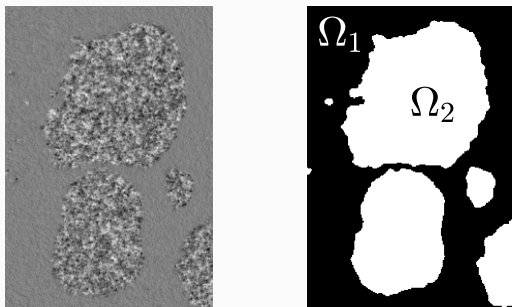


**Crucial** to describe and to process **real-world** images

# Textured image segmentation



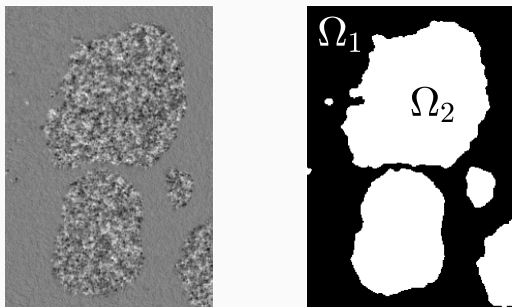
## Textured image segmentation



**Goal:** obtain a partition of the image into  $L$  homogeneous textures

$$\Omega = \Omega_1 \sqcup \dots \sqcup \Omega_L$$

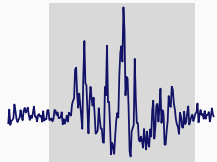
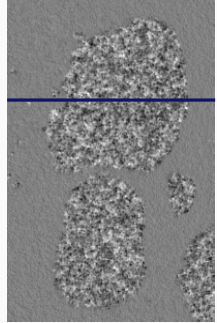
## Textured image segmentation



**Goal:** obtain a partition of the image into  $L$  **homogeneous textures**

$$\Omega = \Omega_1 \sqcup \dots \sqcup \Omega_L$$

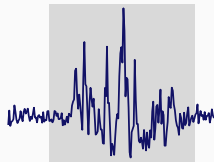
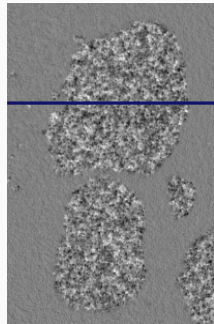
# Features describing fractal textures



# Features describing fractal textures

## Fractals attributes

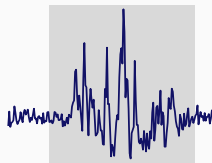
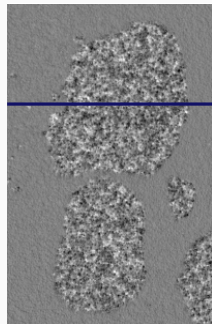
- variance  $\sigma^2$      *amplitude of variations*



# Features describing fractal textures

## Fractals attributes

- variance  $\sigma^2$       *amplitude of variations*
- local regularity  $h$       *scale invariance*

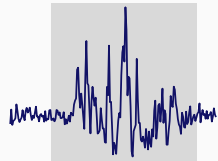
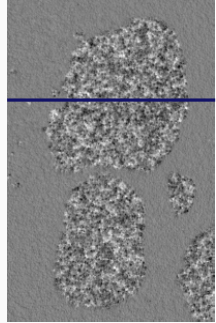


# Features describing fractal textures

## Fractals attributes

- variance  $\sigma^2$       *amplitude of variations*
- local regularity  $h$       *scale invariance*

$$|f(\underline{x}) - f(\underline{y})| \leq \sigma(\underline{x}) |\underline{x} - \underline{y}|^{h(\underline{x})}$$



# Features describing fractal textures

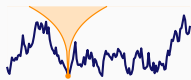
## Fractals attributes

- variance  $\sigma^2$       *amplitude of variations*
- local regularity  $h$       *scale invariance*

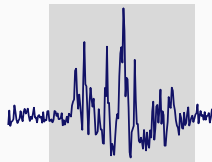
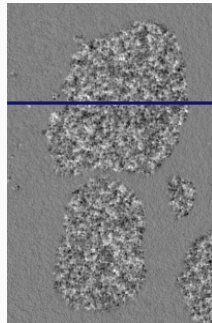
$$|f(\underline{x}) - f(\underline{y})| \leq \sigma(\underline{x}) |\underline{x} - \underline{y}|^{h(\underline{x})}$$



$$h(\underline{x}) \equiv H_1 = 0.9$$



$$h(\underline{x}) \equiv H_2 = 0.3$$



# Features describing fractal textures

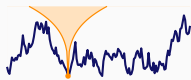
## Fractals attributes

- variance  $\sigma^2$       *amplitude of variations*
- local regularity  $h$       *scale invariance*

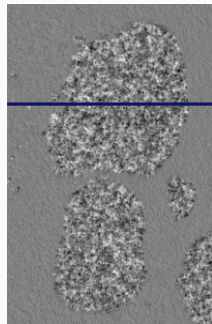
$$|f(\underline{x}) - f(\underline{y})| \leq \sigma(\underline{x}) |\underline{x} - \underline{y}|^{h(\underline{x})}$$



$$h(\underline{x}) \equiv H_1 = 0.9$$

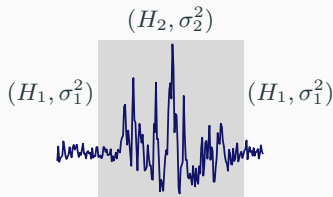


$$h(\underline{x}) \equiv H_2 = 0.3$$



## Segmentation

- ▶  $h$  and  $\sigma^2$  piecewise constant



# Features describing fractal textures

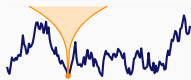
## Fractals attributes

- variance  $\sigma^2$       *amplitude of variations*
- local regularity  $h$       *scale invariance*

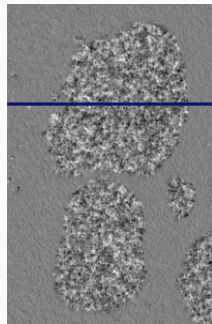
$$|f(\underline{x}) - f(\underline{y})| \leq \sigma(\underline{x}) |\underline{x} - \underline{y}|^{h(\underline{x})}$$



$$h(\underline{x}) \equiv H_1 = 0.9$$

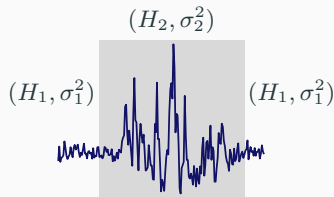


$$h(\underline{x}) \equiv H_2 = 0.3$$



## Segmentation

- ▶  $h$  and  $\sigma^2$  piecewise constant
- ▶ region  $\Omega_k$  characterized by  $(H_k, \sigma_k^2)$



## Self-similar Gaussian Fields: a few models

Let  $H \in (0, 1)$  be a so-called **Hurst index**;  $\sigma^2 > 0$  a variance;  
 $\tilde{W}$  the Fourier transform of a Wiener measure.

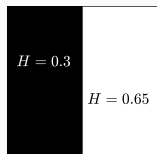
# Self-similar Gaussian Fields: a few models

Let  $H \in (0, 1)$  be a so-called **Hurst index**;  $\sigma^2 > 0$  a variance;

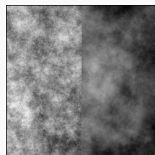
$\tilde{W}$  the Fourier transform of a Wiener measure.

- **Fractional Brownian Field** 
$$B_H(\underline{x}) = \frac{\sigma}{\sqrt{C_H}} \int_{\mathbb{R}^2} \frac{e^{-i\langle \underline{x}, \underline{\xi} \rangle} - 1}{\|\underline{\xi}\|^{H+1}} \tilde{W}(d\underline{\xi})$$

[B. B. Mandelbrot & J. W. Van Ness, 1968, *SIAM Rev.*]



mask



fBf  $B_H$

# Self-similar Gaussian Fields: a few models

Let  $H \in (0, 1)$  be a so-called **Hurst index**;  $\sigma^2 > 0$  a variance;

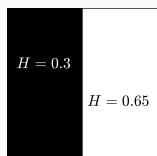
$\tilde{W}$  the Fourier transform of a Wiener measure.

- **Fractional Brownian Field** 
$$B_H(\underline{x}) = \frac{\sigma}{\sqrt{C_H}} \int_{\mathbb{R}^2} \frac{e^{-i\langle \underline{x}, \underline{\xi} \rangle} - 1}{\|\underline{\xi}\|^{H+1}} \tilde{W}(d\underline{\xi})$$

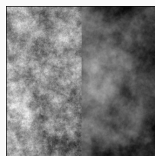
[B. B. Mandelbrot & J. W. Van Ness, 1968, *SIAM Rev.*]

- **Fractional Gaussian Field** [B. Pascal et al., 2021, *Appl. Comp. Harmon. Anal.*]

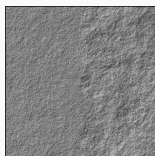
$$G_H(\underline{x}) = \frac{1}{2} \underbrace{(B_H(\underline{x} + \underline{e}_1) - B_H(\underline{x}))}_{\text{horizontal increment}} + \frac{1}{2} \underbrace{(B_H(\underline{x} + \underline{e}_2) - B_H(\underline{x}))}_{\text{vertical increment}}$$



mask



fBf  $B_H$



fGf  $G_H$

# Self-similar Gaussian Fields: a few models

Let  $H \in (0, 1)$  be a so-called **Hurst index**;  $\sigma^2 > 0$  a variance;

$\tilde{W}$  the Fourier transform of a Wiener measure.

- **Fractional Brownian Field** 
$$B_H(\underline{x}) = \frac{\sigma}{\sqrt{C_H}} \int_{\mathbb{R}^2} \frac{e^{-i\langle \underline{x}, \underline{\xi} \rangle} - 1}{\|\underline{\xi}\|^{H+1}} \tilde{W}(d\underline{\xi})$$

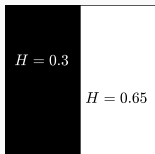
[B. B. Mandelbrot & J. W. Van Ness, 1968, *SIAM Rev.*]

- **Fractional Gaussian Field** [B. Pascal et al., 2021, *Appl. Comp. Harmon. Anal.*]

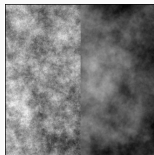
$$G_H(\underline{x}) = \frac{1}{2} \underbrace{(B_H(\underline{x} + \underline{e}_1) - B_H(\underline{x}))}_{\text{horizontal increment}} + \frac{1}{2} \underbrace{(B_H(\underline{x} + \underline{e}_2) - B_H(\underline{x}))}_{\text{vertical increment}}$$

- **Filtered fBf** [B. Pascal et al., 2025, *IEEE Stat. Signal Process.*]

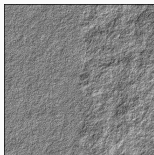
$$C_H(\underline{x}) = \langle B_H, \mathbf{w}_{\underline{x}} \rangle, \text{ w isotropic high-pass filter}$$



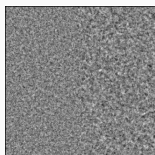
mask



fBf  $B_H$



fGf  $G_H$



Filtered fBf

# Synthetic fractal textures for performance assessment

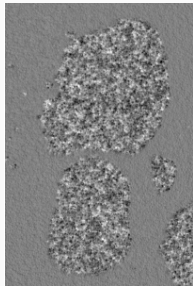
How to choose a model to generate synthetic textures?

# Synthetic fractal textures for performance assessment

## How to choose a model to generate synthetic textures?

- visually resemble real textures: isotropic, stationary

Real

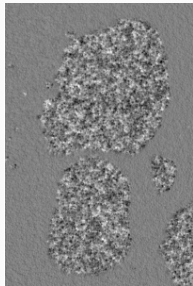


# Synthetic fractal textures for performance assessment

How to choose a model to generate synthetic textures?

- visually resemble real textures: isotropic, stationary
- self-similar field characterized by  $(H, \sigma^2)$  such that  $h(\underline{x}) \equiv H$

Real

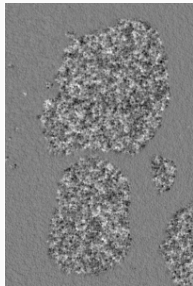


# Synthetic fractal textures for performance assessment

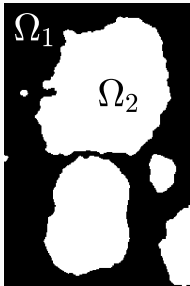
## How to choose a model to generate synthetic textures?

- visually resemble real textures: isotropic, stationary
- self-similar field characterized by  $(H, \sigma^2)$  such that  $h(\underline{x}) \equiv H$
- easy to “patch”: no artifact at the border

Real



Mask

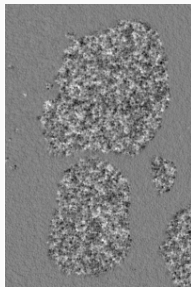


# Synthetic fractal textures for performance assessment

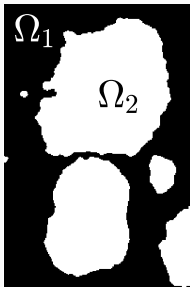
## How to choose a model to generate synthetic textures?

- visually resemble real textures: isotropic, stationary ✓
- self-similar field characterized by  $(H, \sigma^2)$  such that  $h(\underline{x}) \equiv H$  ✓
- easy to “patch”: no artifact at the border ✗

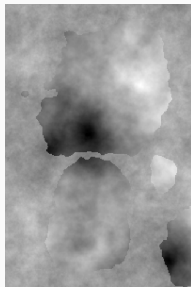
Real



Mask



fBf

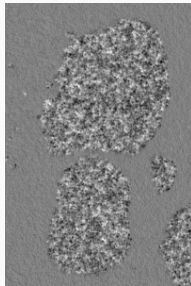


# Synthetic fractal textures for performance assessment

How to choose a model to generate synthetic textures?

- visually resemble real textures: isotropic, stationary ✓
- self-similar field characterized by  $(H, \sigma^2)$  such that  $h(\underline{x}) \equiv H$  ✓
- easy to “patch”: no artifact at the border ✓

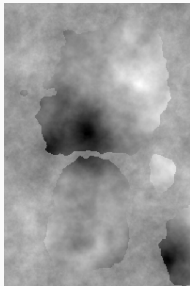
Real



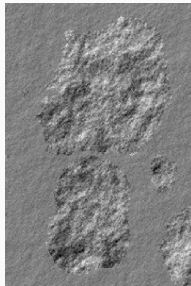
Mask



fBf



fGf



# Multiscale analysis to probe local regularity

Field  $X \in L^2(\mathbb{R}^2)$  and mother wavelet  $\psi$  with  $n_\psi$  **vanishing moments**

**Proposition** If the Hölder local regularity of  $F$  at  $\underline{x}_0$  is  $h(\underline{x}_0) \leq n_\psi$ ,

$$\exists A > 0, \quad |\mathcal{W}_f(\underline{x}, a)| \leq Aa^{h(\underline{x}_0)+1} \left( 1 + \left\| \frac{\underline{x}_0 - \underline{x}}{a} \right\|^{h(\underline{x}_0)} \right)$$

[S. Jaffard, 1991, *Publicacions Matemàtiques*]

# Multiscale analysis to probe local regularity

Field  $X \in L^2(\mathbb{R}^2)$  and mother wavelet  $\psi$  with  $n_\psi$  **vanishing moments**

**Proposition** If the Hölder local regularity of  $F$  at  $\underline{x}_0$  is  $h(\underline{x}_0) \leq n_\psi$ ,

$$\exists A > 0, \quad |\mathcal{W}_f(\underline{x}, a)| \leq Aa^{h(\underline{x}_0)+1} \left( 1 + \left\| \frac{\underline{x}_0 - \underline{x}}{a} \right\|^{h(\underline{x}_0)} \right)$$

[S. Jaffard, 1991, *Publicacions Matemàtiques*]

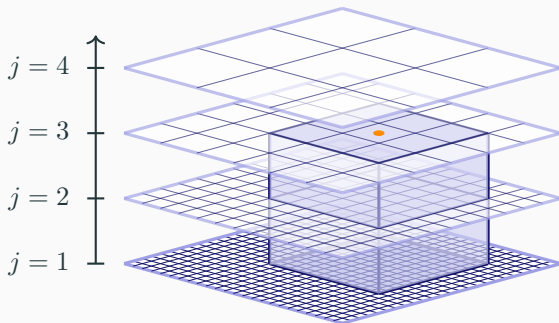
**Discrete wavelet coefficients**  $\zeta_{j,\underline{k}} = \langle X, \psi_{j,\underline{k}} \rangle$  with  $\psi$  an  $L^1$ -normalized

$$|\zeta_{j,\underline{k}}^{(m)}| \lesssim_{2^j \rightarrow 0} \eta(\underline{n}) 2^{jh(\underline{n})}, \quad \text{for } \underline{n} = 2^j \underline{k}$$

with  $\eta(\underline{n})$  some positive-valued function

## Decimated wavelet leader coefficients

$$\tilde{\mathcal{L}}_{j,\underline{k}}[\mathbf{X}] = \sup_{m \in \{1, 2, 3\}} \left| 2^{j\gamma} \zeta_{j',\underline{k}'}^{(m)}[\mathbf{X}] \right|, \text{ with } \begin{cases} \lambda_{j,\underline{n}} = [\underline{k}2^j, (\underline{k} + 1)2^j[ \\ 3\lambda_{j,\underline{n}} = \bigcup_{\underline{p} \in \{-1,0,1\}^2} \lambda_{j,\underline{k}+\underline{p}}, \\ \lambda_{j',\underline{n}'} \subset 3\lambda_{j,\underline{n}} \end{cases}$$

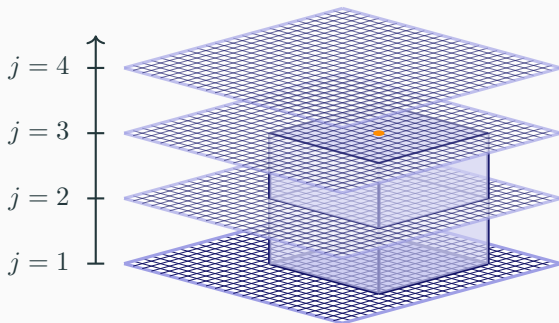


Wavelet  $p$ -Leader and Bootstrap based MultiFractal analysis (PLBMF)

[irit.fr/~Herwig.Wendt/software](http://irit.fr/~Herwig.Wendt/software)

## Undecimated wavelet leader coefficients

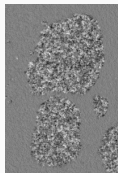
$$\mathcal{L}_{j,\underline{n}}[X] = \sup_{m \in \{1, 2, 3\}} \left| 2^{j\gamma} \zeta_{j',\underline{n}'}^{(m)}[X] \right|, \text{ with } \begin{cases} \lambda_{j,\underline{n}} = [\underline{n}, \underline{n} + 2^j[ \\ 3\lambda_{j,\underline{n}} = \bigcup_{\underline{p} \in \{-2^j, 0, 2^j\}^2} \lambda_{j,\underline{n}+\underline{p}}, \\ \lambda_{j',\underline{n}'} \subset 3\lambda_{j,\underline{n}} \end{cases}$$



[S. Jaffard, 2004, *Proc. Symp. Pure Math.*;  
H. Wendt et al., 2008, *IEEE T. Signal Proces.*]

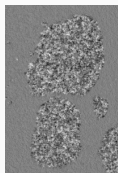
# Multiscale analysis

Textured image

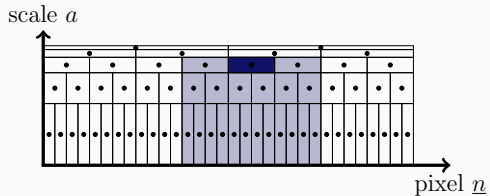


# Multiscale analysis

Textured image

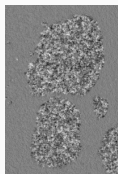


Local maximum of wavelet coefficients:  $\mathcal{L}_a$ .



# Multiscale analysis

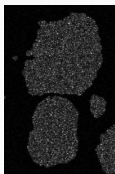
Textured image



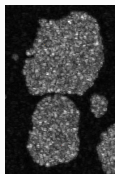
Local maximum of wavelet coefficients:  $\mathcal{L}_a$ .

Scale

$a = 2^1$

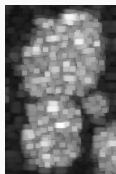


$a = 2^2$

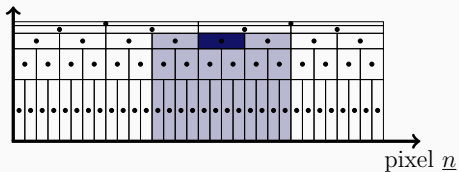


...

$a = 2^5$

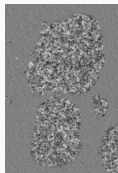


scale  $a$



# Multiscale analysis

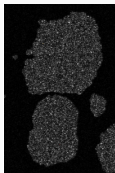
Textured image



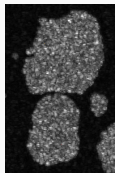
Local maximum of wavelet coefficients:  $\mathcal{L}_a$ .

Scale

$a = 2^1$

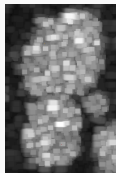


$a = 2^2$



...

$a = 2^5$



## Proposition

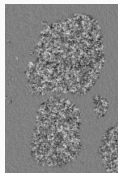
$$\log(\mathcal{L}_a) \underset{a \rightarrow 0}{\simeq} \log(a) \underset{\text{regularity}}{h} + \underset{\substack{\propto \log(\sigma^2) \\ \text{(variance)}}}{v}$$

[S. Jaffard, 2004, *Proc. Symp. Pure Math.*;

H. Wendt et al., 2008, *IEEE T. Signal Proces.*]

# Multiscale analysis

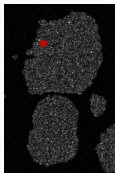
Textured image



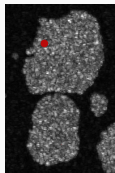
Local maximum of wavelet coefficients:  $\mathcal{L}_{a,\cdot}$

Scale

$a = 2^1$

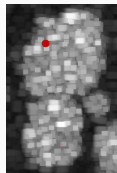


$a = 2^2$



...

$a = 2^5$

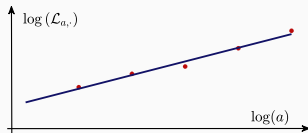


## Proposition

$$\log(\mathcal{L}_{a,\cdot}) \underset{a \rightarrow 0}{\simeq} \log(a) \underset{\text{regularity}}{h} + \underset{\substack{\propto \log(\sigma^2) \\ \text{(variance)}}}{v}$$

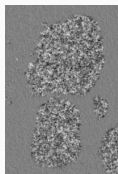
[S. Jaffard, 2004, *Proc. Symp. Pure Math.*;

H. Wendt et al., 2008, *IEEE T. Signal Proces.*]



# Multiscale analysis

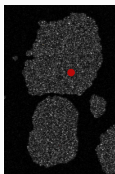
Textured image



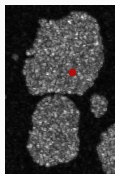
Local maximum of wavelet coefficients:  $\mathcal{L}_{a,\cdot}$ .

Scale

$a = 2^1$

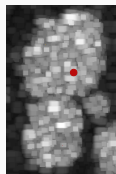


$a = 2^2$



...

$a = 2^5$

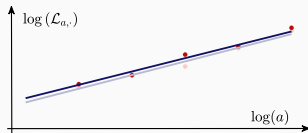


## Proposition

$$\log(\mathcal{L}_{a,\cdot}) \underset{a \rightarrow 0}{\simeq} \log(a) \underset{\text{regularity}}{h} + \underset{\substack{\propto \log(\sigma^2) \\ \text{(variance)}}}{v}$$

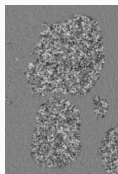
[S. Jaffard, 2004, *Proc. Symp. Pure Math.*;

H. Wendt et al., 2008, *IEEE T. Signal Proces.*]



# Multiscale analysis

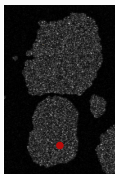
Textured image



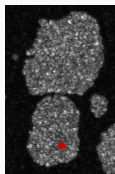
Local maximum of wavelet coefficients:  $\mathcal{L}_{a,\cdot}$ .

Scale

$a = 2^1$

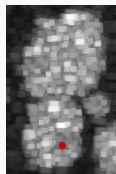


$a = 2^2$



...

$a = 2^5$

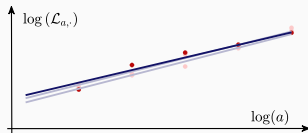


## Proposition

$$\log(\mathcal{L}_{a,\cdot}) \underset{a \rightarrow 0}{\simeq} \log(a) \underset{\text{regularity}}{h} + \underset{\substack{\propto \log(\sigma^2) \\ \text{(variance)}}}{v}$$

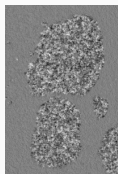
[S. Jaffard, 2004, *Proc. Symp. Pure Math.*;

H. Wendt et al., 2008, *IEEE T. Signal Proces.*]



# Multiscale analysis

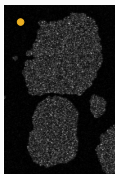
Textured image



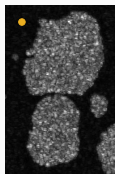
Local maximum of wavelet coefficients:  $\mathcal{L}_{a,\cdot}$

Scale

$a = 2^1$

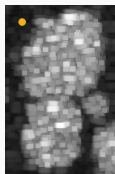


$a = 2^2$



...

$a = 2^5$

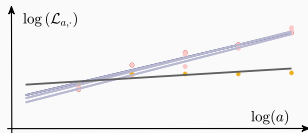


## Proposition

$$\log(\mathcal{L}_{a,\cdot}) \underset{a \rightarrow 0}{\simeq} \log(a) \underset{\text{regularity}}{h} + \underset{\substack{\propto \log(\sigma^2) \\ \text{(variance)}}}{v}$$

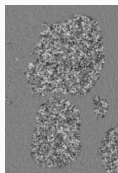
[S. Jaffard, 2004, *Proc. Symp. Pure Math.*;

H. Wendt et al., 2008, *IEEE T. Signal Proces.*]



# Multiscale analysis

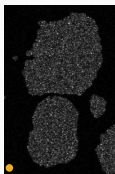
Textured image



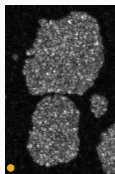
Local maximum of wavelet coefficients:  $\mathcal{L}_{a,\cdot}$

Scale

$a = 2^1$

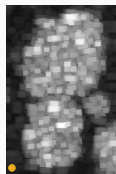


$a = 2^2$



...

$a = 2^5$

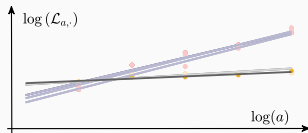


## Proposition

$$\log(\mathcal{L}_{a,\cdot}) \underset{a \rightarrow 0}{\simeq} \log(a) \underset{\text{regularity}}{h} + \underset{\substack{\propto \log(\sigma^2) \\ \text{(variance)}}}{v}$$

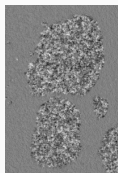
[S. Jaffard, 2004, *Proc. Symp. Pure Math.*;

H. Wendt et al., 2008, *IEEE T. Signal Proces.*]



# Multiscale analysis

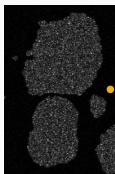
Textured image



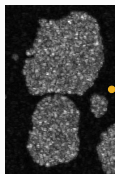
Local maximum of wavelet coefficients:  $\mathcal{L}_{a,\cdot}$

Scale

$a = 2^1$

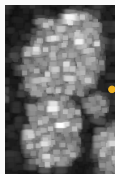


$a = 2^2$



...

$a = 2^5$

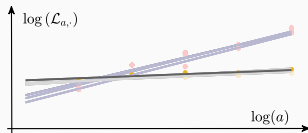


## Proposition

$$\log(\mathcal{L}_{a,\cdot}) \underset{a \rightarrow 0}{\simeq} \log(a) \underset{\text{regularity}}{h} + \underset{\substack{\propto \log(\sigma^2) \\ \text{(variance)}}}{v}$$

[S. Jaffard, 2004, *Proc. Symp. Pure Math.*;

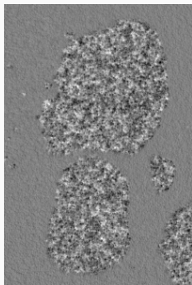
H. Wendt et al., 2008, *IEEE T. Signal Proces.*]



# Direct punctual estimation

**Linear regression**      $\log(\mathcal{L}_{a,\cdot}) \simeq \log(a) \underset{\text{regularity}}{h} + \underset{\propto \log(\sigma^2)}{v}$

Textured image

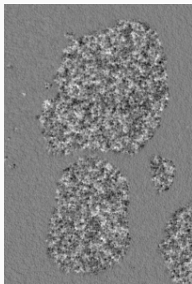


# Direct punctual estimation

**Linear regression**  $\log(\mathcal{L}_{a,\cdot}) \simeq \log(a) \underset{\text{regularity}}{h} + \underset{\propto \log(\sigma^2)}{v}$

$$\left(\hat{h}^{\text{LR}}, \hat{v}^{\text{LR}}\right) = \underset{h,v}{\operatorname{argmin}} \sum_{a=a_{\min}}^{a_{\max}} \|\log(\mathcal{L}_{a,\cdot}) - \log(a)h - v\|^2$$

Textured image

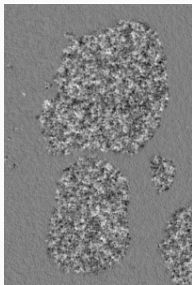


# Direct punctual estimation

**Linear regression**  $\log(\mathcal{L}_{a,\cdot}) \simeq \log(a) \underset{\text{regularity}}{h} + \underset{\propto \log(\sigma^2)}{v}$

$$\left(\hat{h}^{\text{LR}}, \hat{v}^{\text{LR}}\right) = \underset{h,v}{\operatorname{argmin}} \sum_{a=a_{\min}}^{a_{\max}} \|\log(\mathcal{L}_{a,\cdot}) - \log(a)h - v\|^2$$

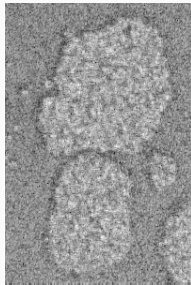
Textured image



Local regularity  $\hat{h}^{\text{LR}}$



Local power  $\hat{v}^{\text{LR}}$

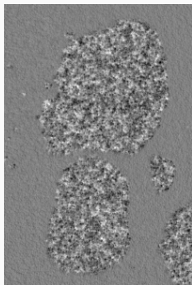


# Direct punctual estimation

**Linear regression**  $\frac{\mathbb{E} \log(\mathcal{L}_{a,\cdot})}{\text{expected value}} = \log(a) \underset{\text{regularity}}{\bar{h}} + \underset{\propto \log(\sigma^2)}{\bar{v}}$

$$\left( \hat{h}^{\text{LR}}, \hat{v}^{\text{LR}} \right) = \underset{h, v}{\operatorname{argmin}} \sum_{a=a_{\min}}^{a_{\max}} \|\log(\mathcal{L}_{a,\cdot}) - \log(a)h - v\|^2$$

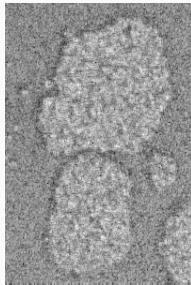
Textured image



Local regularity  $\hat{h}^{\text{LR}}$

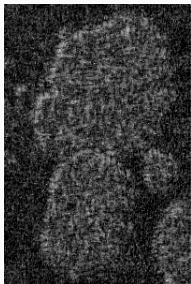


Local power  $\hat{v}^{\text{LR}}$



# *A posteriori* regularization

Linear regression  $\hat{h}^{\text{LR}}$



## *A posteriori* regularization

**Finite differences**  $D_{1h}$  (horizontal),  $D_{2h}$  (vertical) in each pixel

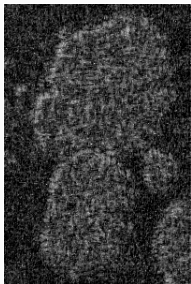
Linear regression  $\hat{h}^{LR}$



# A *posteriori* regularization

**Finite differences**  $D_h = [D_1 h, D_2 h]$

Linear regression  $\hat{h}^{\text{LR}}$



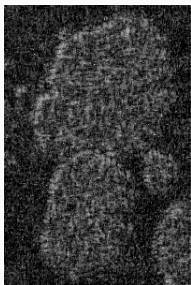
# A posteriori regularization

**Finite differences**  $Dh = [D_1h, D_2h]$

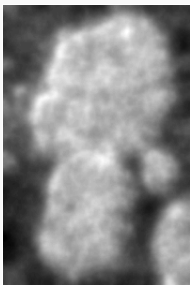
**Filter smoothing** (linear)

$$\begin{aligned} \operatorname{argmin}_h \quad & \|h - \hat{h}^{\text{LR}}\|^2 + \theta \|Dh\|_2^2 \\ & = (I + \theta D^\top D)^{-1} \hat{h}^{\text{LR}} \end{aligned}$$

Linear regression  $\hat{h}^{\text{LR}}$



Smoothing



# A posteriori regularization

**Finite differences**  $Dh = [D_1h, D_2h]$

**Filter smoothing** (linear)

$$\begin{aligned} \operatorname{argmin}_h \|h - \hat{h}^{\text{LR}}\|^2 + \theta \|Dh\|_2^2 \\ = (I + \theta D^\top D)^{-1} \hat{h}^{\text{LR}} \end{aligned}$$

**ROF denoising** (nonlinear)

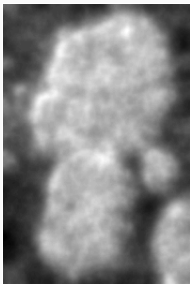
$$\operatorname{argmin}_h \|h - \hat{h}^{\text{LR}}\|^2 + \theta \|Dh\|_{2,1}$$

[F. Abboud et al., 2017, *J. Math. Imaging Vis.*]

Linear regression  $\hat{h}^{\text{LR}}$



Smoothing



ROF



# A posteriori regularization

**Finite differences**  $Dh = [D_1h, D_2h]$

**Filter smoothing** (linear)

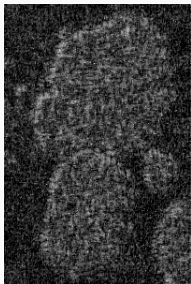
$$\begin{aligned} \operatorname{argmin}_h \|h - \hat{h}^{\text{LR}}\|^2 + \theta \|Dh\|_2^2 \\ = (I + \theta D^\top D)^{-1} \hat{h}^{\text{LR}} \end{aligned}$$

**ROF denoising** (nonlinear)

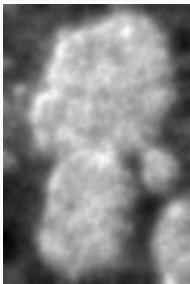
$$\operatorname{argmin}_h \|h - \hat{h}^{\text{LR}}\|^2 + \theta \|Dh\|_{2,1}$$

[F. Abboud et al., 2017, *J. Math. Imaging Vis.*]

Linear regression  $\hat{h}^{\text{LR}}$



Smoothing



ROF

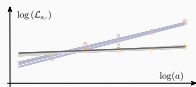


→ cumulative estimation variance and regularization bias

## Functionals with either free or co-localized contours

$$\sum_a \frac{\|\log \mathcal{L}_{a,..} - \log(a)h - v\|^2}{\text{Least-Squares}}$$

→ fidelity to the log-linear model

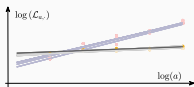


# Functionals with either free or co-localized contours

$$\sum_a \frac{\|\log \mathcal{L}_{a,\cdot} - \log(a)h - v\|^2}{\text{Least-Squares}} + \theta_1 \frac{\mathcal{Q}(Dh, Dv; \theta_2)}{\text{Total Variation}}$$

→ fidelity to the log-linear model

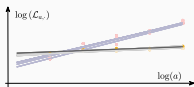
→ favors piecewise constancy



# Functionals with either free or co-localized contours

$$\underset{h,v}{\text{minimize}} \sum_a \frac{\|\log \mathcal{L}_{a,\cdot} - \log(a)h - v\|^2}{\text{Least-Squares}} + \theta_1 \frac{\mathcal{Q}(Dh, Dv; \theta_2)}{\text{Total Variation}}$$

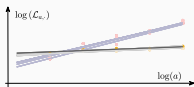
$\rightarrow$  fidelity to the log-linear model                       $\rightarrow$  favors piecewise constancy



# Functionals with either free or co-localized contours

$$\underset{h,v}{\text{minimize}} \sum_a \frac{\|\log \mathcal{L}_{a,\cdot} - \log(a)h - v\|^2}{\text{Least-Squares}} + \theta_1 \frac{\mathcal{Q}(Dh, Dv; \theta_2)}{\text{Total Variation}}$$

$\rightarrow$  fidelity to the log-linear model  $\rightarrow$  favors piecewise constancy

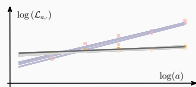


**Finite differences**  $D_1h$  (horizontal),  $D_2h$  (vertical) in each pixel

# Functionals with either free or co-localized contours

$$\underset{h,v}{\text{minimize}} \sum_a \frac{\|\log \mathcal{L}_{a,\cdot} - \log(a)h - v\|^2}{\text{Least-Squares}} + \theta_1 \frac{\mathcal{Q}(\text{D}h, \text{D}v; \theta_2)}{\text{Total Variation}}$$

$\rightarrow$  fidelity to the log-linear model  $\rightarrow$  favors piecewise constancy



**Finite differences**  $\text{D}h = [\text{D}_1 h, \text{D}_2 h]$

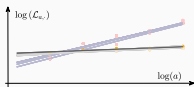
Free:  $h, v$  are **independently** piecewise constant

$$\mathcal{Q}_F(\text{D}h, \text{D}v; \theta_2) = \theta_2 \|\text{D}h\|_{2,1} + \|\text{D}v\|_{2,1}$$

# Functionals with either free or co-localized contours

$$\underset{h,v}{\text{minimize}} \sum_a \frac{\|\log \mathcal{L}_{a,\cdot} - \log(a)h - v\|^2}{\text{Least-Squares}} + \theta_1 \frac{\mathcal{Q}(\text{D}h, \text{D}v; \theta_2)}{\text{Total Variation}}$$

$\rightarrow$  fidelity to the log-linear model  $\rightarrow$  favors piecewise constancy



**Finite differences**  $\text{D}h = [\text{D}_1 h, \text{D}_2 h]$

Free:  $h, v$  are **independently** piecewise constant

$$\mathcal{Q}_F(\text{D}h, \text{D}v; \theta_2) = \theta_2 \|\text{D}h\|_{2,1} + \|\text{D}v\|_{2,1}$$

Co-localized:  $h, v$  are **concomitantly** piecewise constant

$$\mathcal{Q}_C(\text{D}h, \text{D}v; \theta_2) = \|[\theta_2 \text{D}h, \text{D}v]\|_{2,1}$$

# Functionals minimization

$$\underset{h,v}{\text{minimize}} \quad \sum_a \frac{\|\log \mathcal{L}_{a,\cdot} - \log(a)h - v\|^2}{\text{Least-Squares}} \quad + \quad \theta_1 \frac{\mathcal{Q}(Dh, Dv; \theta_2)}{\text{Total Variation}}$$



# Functionals minimization

$$\underset{h,v}{\text{minimize}} \quad \sum_a \frac{\|\log \mathcal{L}_{a,\cdot} - \log(a)h - v\|^2}{\text{Least-Squares}} \quad + \quad \theta_1 \frac{\mathcal{Q}(\text{D}h, \text{D}v; \theta_2)}{\text{Total Variation}}$$



- gradient descent  $x^{[k+1]} = x^{[k]} - \tau \nabla f(x^{[k]})$   $x = (h, v)$

# Functionals minimization

$$\underset{h,v}{\text{minimize}} \quad \sum_a \frac{\|\log \mathcal{L}_{a,\cdot} - \log(a)h - v\|^2}{\text{Least-Squares}} + \theta_1 \frac{\mathcal{Q}(Dh, Dv; \theta_2)}{\text{Total Variation}}$$



nonsmooth



- ▶ gradient descent  $x^{[k+1]} = x^{[k]} - \tau \nabla f(x^{[k]})$   $x = (h, v)$
- ▶ implicit subgradient descent: proximal point algorithm  
 $x^{[k+1]} = x^{[k]} - \tau u^{[k]}, u^{[k]} \in \partial f(x^{[k+1]}) \Leftrightarrow x^{[k+1]} = \text{prox}_{\tau f}(x^{[k]})$

# Functionals minimization

$$\underset{h,v}{\text{minimize}} \quad \sum_a \frac{\|\log \mathcal{L}_{a,\cdot} - \log(a)h - v\|^2}{\text{Least-Squares}} + \theta_1 \frac{\mathcal{Q}(Dh, Dv; \theta_2)}{\text{Total Variation}}$$



nonsmooth



► gradient descent  $x^{[k+1]} = x^{[k]} - \tau \nabla f(x^{[k]})$   $x = (h, v)$

► implicit subgradient descent: proximal point algorithm

$$x^{[k+1]} = x^{[k]} - \tau u^{[k]}, \quad u^{[k]} \in \partial f(x^{[k+1]}) \Leftrightarrow x^{[k+1]} = \text{prox}_{\tau f}(x^{[k]})$$

► splitting proximal algorithm

$$u^{[k+1]} = \text{prox}_{\sigma(\theta \mathcal{Q})^*} \left( u^{[k]} + \sigma D \bar{x}^{[k]} \right)$$

$$x^{[k+1]} = \text{prox}_{\tau \|\mathcal{L} - A \cdot\|_2^2} \left( x^{[k]} - \tau D^\top u^{[k+1]} \right), \quad A : (h, v) \mapsto \{\log(a)h + v\}_a$$

$$\bar{x}^{[k+1]} = 2x^{[k+1]} - x^{[k]} \quad [\text{A. Chambolle et al., 2011, } J. \text{ Math. Imaging Vis.}]$$

# Functionals minimization

$$\underset{h,v}{\text{minimize}} \quad \sum_a \frac{\|\log \mathcal{L}_{a,\cdot} - \log(a)h - v\|^2}{\text{Least-Squares}} + \theta_1 \frac{\mathcal{Q}(Dh, Dv; \theta_2)}{\text{Total Variation}}$$



nonsmooth



► gradient descent  $x^{[k+1]} = x^{[k]} - \tau \nabla f(x^{[k]})$   $x = (h, v)$

► implicit subgradient descent: proximal point algorithm

$$x^{[k+1]} = x^{[k]} - \tau u^{[k]}, \quad u^{[k]} \in \partial f(x^{[k+1]}) \Leftrightarrow x^{[k+1]} = \text{prox}_{\tau f}(x^{[k]})$$

► splitting proximal algorithm

$$u^{[k+1]} = \text{prox}_{\sigma(\theta \mathcal{Q})^*} \left( u^{[k]} + \sigma D \bar{x}^{[k]} \right)$$

$$x^{[k+1]} = \text{prox}_{\tau \|\mathcal{L} - A \cdot\|_2^2} \left( x^{[k]} - \tau D^\top u^{[k+1]} \right), \quad A : (h, v) \mapsto \{\log(a)h + v\}_a$$

$$\bar{x}^{[k+1]} = 2x^{[k+1]} - x^{[k]} \quad [\text{A. Chambolle et al., 2011, } J. \text{ Math. Imaging Vis.}]$$

# Accelerated algorithm based on strong-convexity

$$\underset{h,v}{\text{minimize}} \quad \sum_a \underbrace{\frac{\|\log \mathcal{L}_{a,\cdot} - \log(a)h - v\|^2}{\text{Least-Squares}}}_{\text{Least-Squares}} + \theta_1 \underbrace{\mathcal{Q}(\text{D}h, \text{D}v; \theta_2)}_{\text{Total Variation}}$$



nonsmooth



Primal-dual algorithm [A. Chambolle et al., 2011, *J. Math. Imaging Vis.*]

$$\delta: \text{duality gap}, \delta(x^{[k]}, u^{[k]}) \xrightarrow{n \rightarrow \infty} 0$$

# Accelerated algorithm based on strong-convexity

$$\underset{h,v}{\text{minimize}} \quad \sum_a \frac{\|\log \mathcal{L}_{a,\cdot} - \log(a)h - v\|^2}{\text{Least-Squares}} + \theta_1 \frac{\mathcal{Q}(Dh, Dv; \theta_2)}{\text{Total Variation}}$$

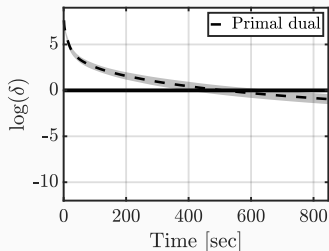


nonsmooth



Primal-dual algorithm [A. Chambolle et al., 2011, *J. Math. Imaging Vis.*]

$\delta$ : duality gap,  $\delta(x^{[k]}, u^{[k]}) \xrightarrow[n \rightarrow \infty]{} 0$



# Convexity properties

$$\underset{h,v}{\text{minimize}} \quad \sum_a \frac{\|\log \mathcal{L}_{a,\cdot} - \log(a)h - v\|^2}{\text{Least-Squares}} + \theta_1 \frac{Q(Dh, Dv; \theta_2)}{\text{Total Variation}}$$



$\rho$ -strongly convex

nonsmooth



# Convexity properties

$$\underset{h,v}{\text{minimize}} \quad \sum_a \frac{\|\log \mathcal{L}_{a,\cdot} - \log(a)h - v\|^2}{\text{Least-Squares}} + \theta_1 \frac{\mathcal{Q}(\text{D}h, \text{D}v; \theta_2)}{\text{Total Variation}}$$



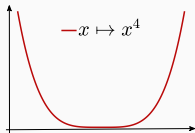
$\rho$ -strongly convex

nonsmooth



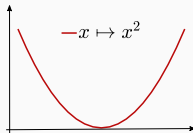
## Strong-convexity

- $f$   $\rho$ -strongly convex iff  $f - \frac{\rho}{2} \|\cdot\|^2$  convex



✓ strictly convex

✗ non strongly convex



✓ strictly convex

✓ 1-strongly convex

# Convexity properties

$$\underset{h,v}{\text{minimize}} \quad \sum_a \frac{\|\log \mathcal{L}_{a,\cdot} - \log(a)h - v\|^2}{\text{Least-Squares}} + \theta_1 \frac{\mathcal{Q}(Dh, Dv; \theta_2)}{\text{Total Variation}}$$



$\rho$ -strongly convex

nonsmooth



## Strong-convexity

- $f$   $\rho$ -strongly convex iff  $f - \frac{\rho}{2} \|\cdot\|^2$  convex
- $f \in \mathcal{C}^2$  with Hessian matrix  $Hf \succeq 0 \implies \rho = \min \text{Sp}(Hf)$

# Convexity properties

$$\underset{h,v}{\text{minimize}} \quad \sum_a \underbrace{\frac{\|\log \mathcal{L}_{a,\cdot} - \log(a)h - v\|^2}{\text{Least-Squares}}}_{\text{Least-Squares}} + \theta_1 \underbrace{\frac{\mathcal{Q}(\text{D}h, \text{D}v; \theta_2)}{\text{Total Variation}}}_{\text{Total Variation}}$$



$\rho$ -strongly convex

nonsmooth



## Strong-convexity

- $f$   $\rho$ -strongly convex iff  $f - \frac{\rho}{2} \|\cdot\|^2$  convex
- $f \in \mathcal{C}^2$  with Hessian matrix  $\text{H}f \succeq 0 \implies \rho = \min \text{Sp}(\text{H}f)$

**Proposition**  $\sum_a \|\log \mathcal{L} - \log(a)h - v\|^2$  is  $\rho$ -strongly convex.

$a_{\min} = 2^1,$	$a_{\max}$	$2^2$	$2^3$	$2^4$	$2^5$	$2^6$
$\rho = \min \text{Sp} (2A^\top A)$	0.29	<b>0.72</b>	1.20	1.69	2.20	

[B. Pascal et al., 2021, *Appl. Comput. Harmon. Anal.*]

# Accelerated algorithm based on strong-convexity

$$\underset{h,v}{\text{minimize}} \quad \sum_a \frac{\|\log \mathcal{L}_{a,\cdot} - \log(a)h - v\|^2}{\text{Least-Squares}} + \theta_1 \frac{\mathcal{Q}(Dh, Dv; \theta_2)}{\text{Total Variation}}$$



$\rho$ -strongly convex

nonsmooth



**Accelerated Primal-dual algorithm** [A. Chambolle et al., 2011, *J. Math. Imaging Vis.*]

**for**  $k = 0, 1, \dots$

$x = (h, v)$

$$u^{[k+1]} = \text{prox}_{\sigma_k(\theta\mathcal{Q})^*} \left( u^{[k]} + \sigma_k D\bar{x}^{[k]} \right)$$

$$x^{[k+1]} = \text{prox}_{\tau_k \|\mathcal{L}-A\cdot\|_2^2} \left( x^{[k]} - \tau_k D^\top u^{[k+1]} \right)$$

$$\theta_k = \sqrt{1 + 2\rho\tau_k}, \quad \tau_{n+1} = \tau_k/\theta_k, \quad \sigma_{n+1} = \theta_k\sigma_k$$

$$\bar{x}^{[k+1]} = x^{[k+1]} + \theta_k^{-1} \left( x^{[k+1]} - x^{[k]} \right)$$

# Accelerated algorithm based on strong-convexity

$$\underset{h,v}{\text{minimize}} \quad \sum_a \frac{\|\log \mathcal{L}_{a,\cdot} - \log(a)h - v\|^2}{\text{Least-Squares}} + \theta_1 \frac{\mathcal{Q}(Dh, Dv; \theta_2)}{\text{Total Variation}}$$



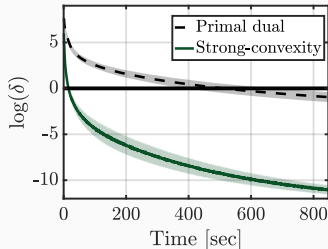
$\rho$ -strongly convex

nonsmooth



**Accelerated Primal-dual algorithm** [A. Chambolle et al., 2011, *J. Math. Imaging Vis.*]

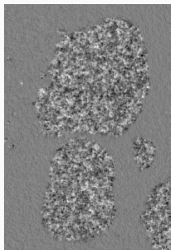
$\delta$ : duality gap,  $\delta(x^{[k]}, u^{[k]}) \xrightarrow[n \rightarrow \infty]{} 0$



# Segmentation *via* iterated thresholding

$$\underset{h,v}{\text{minimize}} \quad \sum_a \frac{\|\log \mathcal{L}_{a,\cdot} - \log(a)h - v\|^2}{\text{Least-Squares}} + \theta_1 \frac{Q(Dh, Dv; \theta_2)}{\text{Total Variation}}$$

Textured image    Lin. reg.  $\hat{h}^{\text{LR}}$



# Segmentation *via* iterated thresholding

$$\underset{h,v}{\text{minimize}} \quad \sum_a \frac{\|\log \mathcal{L}_{a,\cdot} - \log(a)h - v\|^2}{\text{Least-Squares}} + \theta_1 \frac{\mathcal{Q}(Dh, Dv; \theta_2)}{\text{Total Variation}}$$

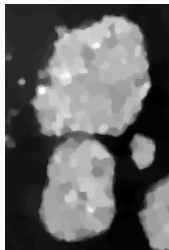
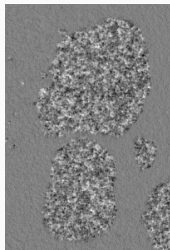
Textured image

Lin. reg.  $\hat{h}^{\text{LR}}$

Co-localized  
contours  $\hat{h}^{\text{C}}$

Threshold  
estimate<sup>†</sup>  $T\hat{h}^{\text{C}}$

[B. Pascal et al., 2021, *Appl. Comput. Harmon. Anal.*]



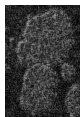
<sup>†</sup>Thresholding strategy from: [X. Cai et al., 2013, *EMMCVPR*]

## Threshold-ROF on $\hat{h}^{LR}$

[C. Naornita et al., 2014, *ICIP*; N. Pustelnik et al., 2016, *IEEE Trans. Comput. Imaging*]

$$\operatorname{argmin}_h \|h - \hat{h}^{LR}\|^2 + \theta \|Dh\|_{2,1}$$

Lin. reg.



ROF



Threshold



Only based on regularity  $h$ .

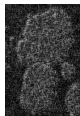
# State-of-the-art methods for texture segmentation

## Threshold-ROF on $\hat{h}^{LR}$

[C. Naornita et al., 2014, *ICIP*; N. Pustelnik et al., 2016, *IEEE Trans. Comput. Imaging*]

$$\operatorname{argmin}_h \|\mathbf{h} - \hat{\mathbf{h}}^{LR}\|^2 + \theta \|\mathbf{D}\mathbf{h}\|_{2,1}$$

Lin. reg.



ROF



Threshold

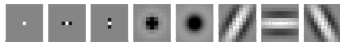


Only based on regularity  $h$ .

## Factorization based segmentation<sup>†</sup>

[J. Yuan, 2015, *IEEE Trans. Image Process.*]

(i) local histograms



(ii) matrix factorization

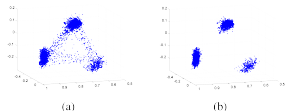


Fig. 2. Scatterplot of features in subspace. (a) Scatterplot of features projected onto the 3-d subspace. (b) Scatterplot after removing features with high edginess.

<sup>†</sup><https://sites.google.com/site/factorizationsegmentation/>

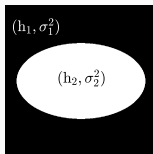
# Compared segmentation performance on synthetic textures

## Piecewise monofractal texture synthesis

[B. Pascal et al., 2021, *Appl. Comput. Harmon. Anal.*]

mask:  $\Omega = \Omega_1 \sqcup \Omega_2$ ,

attributes:  $(H_\ell, \sigma_\ell^2)_{\ell=1,2}$



# Compared segmentation performance on synthetic textures

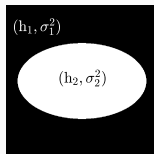
## Piecewise monofractal texture synthesis

[B. Pascal et al., 2021, *Appl. Comput. Harmon. Anal.*]

mask:  $\Omega = \Omega_1 \sqcup \Omega_2$ ,

attributes:  $(H_\ell, \sigma_\ell^2)_{\ell=1,2}$

**Ex.**  $H_1 = 0.5, \sigma_1^2 = 0.6$   
 $H_2 = 0.6, \sigma_2^2 = 0.7$



# Compared segmentation performance on synthetic textures

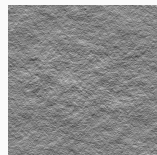
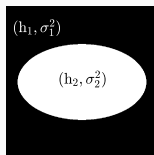
## Piecewise monofractal texture synthesis

[B. Pascal et al., 2021, *Appl. Comput. Harmon. Anal.*]

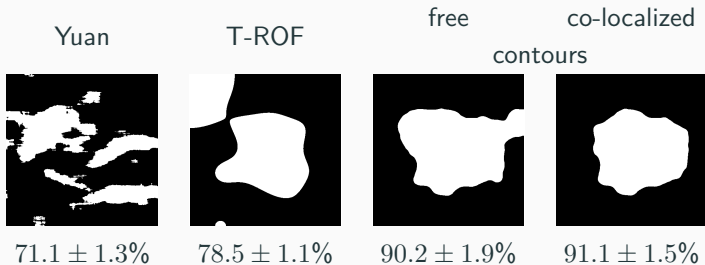
mask:  $\Omega = \Omega_1 \sqcup \Omega_2$ ,

attributes:  $(H_\ell, \sigma_\ell^2)_{\ell=1,2}$

**Ex.**  $H_1 = 0.5, \sigma_1^2 = 0.6$   
 $H_2 = 0.6, \sigma_2^2 = 0.7$

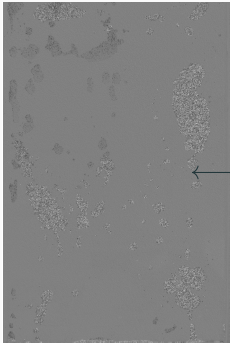


## Averaged segmentation performances over 5 realizations

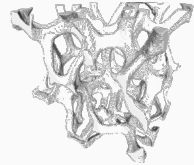


# Multiphase flow through porous media

Laboratoire de Physique, ENS Lyon, V. Vidal, T. Busser, (M. Serres, IFPEN)

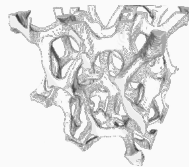
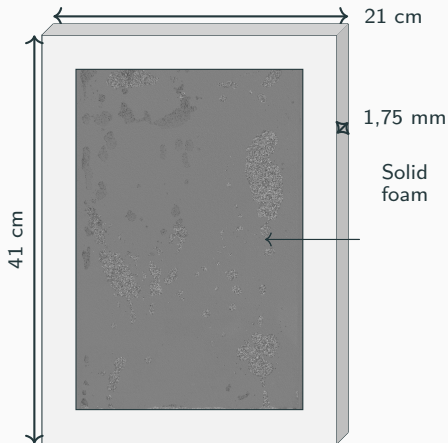


Solid  
foam



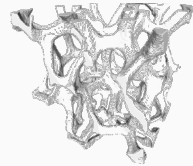
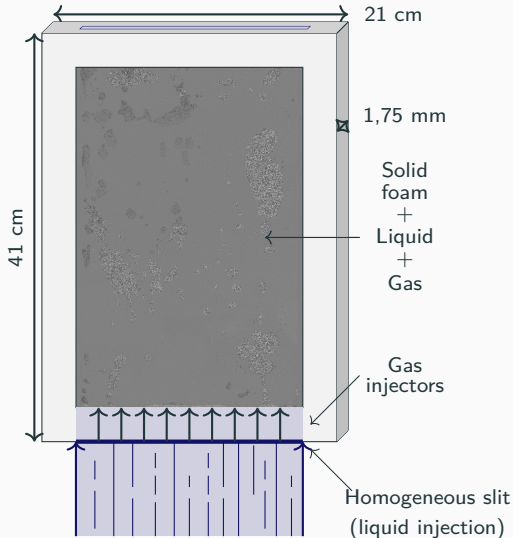
# Multiphase flow through porous media

Laboratoire de Physique, ENS Lyon, V. Vidal, T. Busser, (M. Serres, IFPEN)



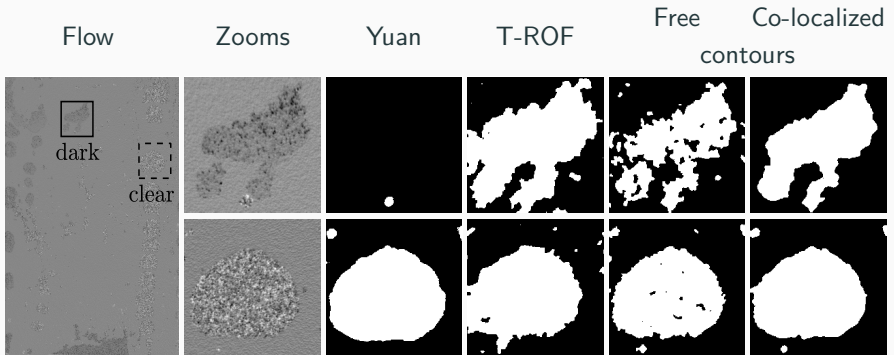
# Multiphase flow through porous media

Laboratoire de Physique, ENS Lyon, V. Vidal, T. Busser, (M. Serres, IFPEN)

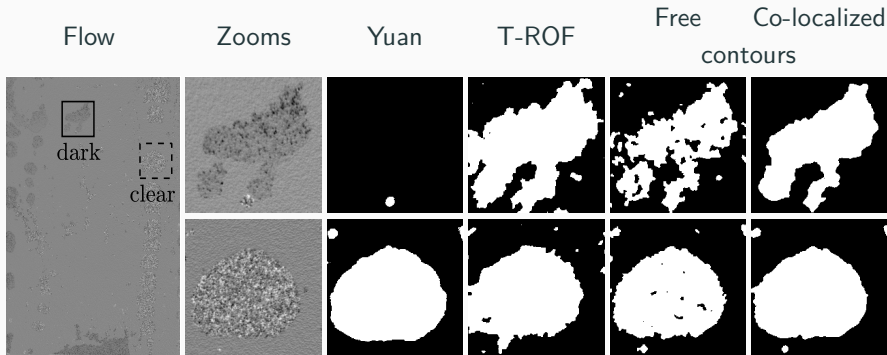


- 1600 × 1100 pixels
  - video: ~ 1000 images
  - phase diagram: ~ 10 flow rates
- rates

Low activity:  $Q_G = 300\text{mL}/\text{min} - Q_L = 300\text{mL}/\text{min}$



Low activity:  $Q_G = 300\text{mL}/\text{min} - Q_L = 300\text{mL}/\text{min}$



Liquid:  $H_L = 0.4$

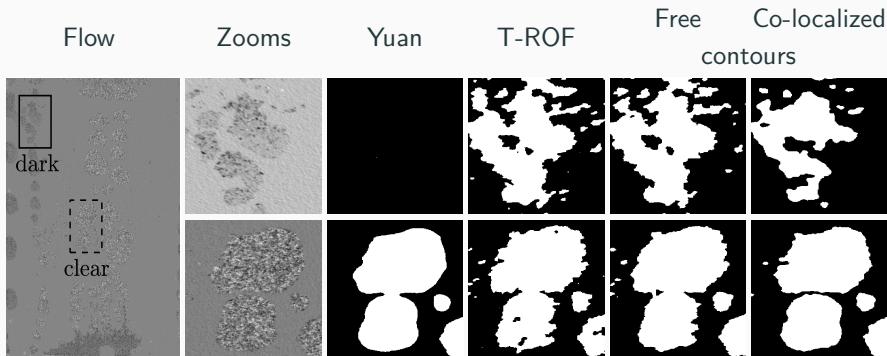
$$\sigma_{\text{dark}}^2 = 10^{-2}$$

Gas:  $H_G = 0.9$

$$\sigma_{\text{dark}}^2 = 10^{-2} \quad (\text{dark bubbles})$$

$$\sigma_{\text{clear}}^2 = 10^{-1} \quad (\text{clear bubbles})$$

Transition:  $Q_G = 400\text{mL}/\text{min} - Q_L = 700\text{mL}/\text{min}$



Liquid:  $H_L = 0.4$

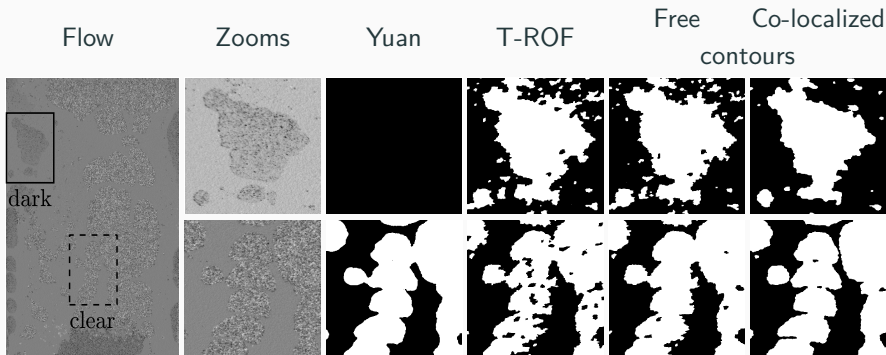
$$\sigma_{\text{dark}}^2 = 10^{-2}$$

Gas:  $H_G = 0.9$

$$\sigma_{\text{dark}}^2 = 10^{-2} \quad (\text{dark bubbles})$$

$$\sigma_{\text{clear}}^2 = 10^{-1} \quad (\text{clear bubbles})$$

High activity:  $Q_G = 1200\text{mL}/\text{min} - Q_L = 300\text{mL}/\text{min}$



Liquid:  $H_L = 0.4$

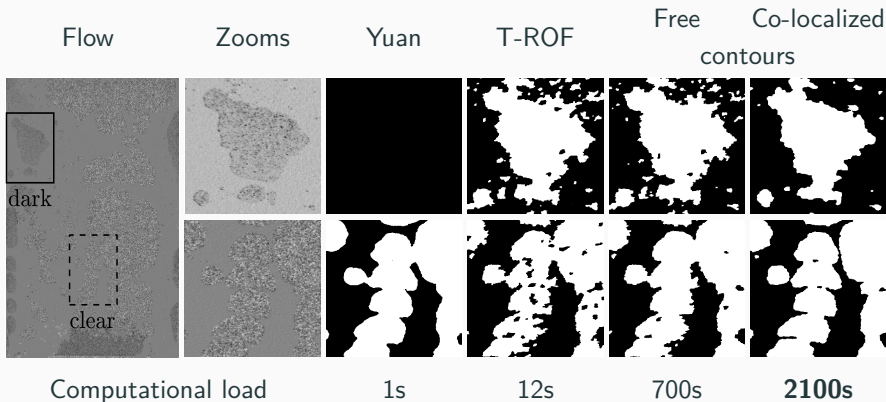
$$\sigma_{\text{dark}}^2 = 10^{-2}$$

Gas:  $H_G = 0.9$

$$\sigma_{\text{dark}}^2 = 10^{-2} \quad (\text{dark bubbles})$$

$$\sigma_{\text{clear}}^2 = 10^{-1} \quad (\text{clear bubbles})$$

# High activity: $Q_G = 1200\text{mL}/\text{min} - Q_L = 300\text{mL}/\text{min}$



Liquid:  $H_L = 0.4$

$$\sigma_{\text{dark}}^2 = 10^{-2}$$

Gas:  $H_G = 0.9$

$$\sigma_{\text{dark}}^2 = 10^{-2} \quad (\text{dark bubbles})$$

$$\sigma_{\text{clear}}^2 = 10^{-1} \quad (\text{clear bubbles})$$

## Regularization parameters selection

$$\left(\hat{h}, \hat{v}\right) (\mathcal{L}; \Theta) = \underset{h, v}{\operatorname{argmin}} \sum_a \|\log \mathcal{L}_{a, \cdot} - \log(a)h - v\|^2 + \theta_1 Q(Dh, Dv; \theta_2)$$

## Regularization parameters selection

$$\left(\hat{h}, \hat{v}\right) (\mathcal{L}; \Theta) = \underset{h, v}{\operatorname{argmin}} \sum_a \|\log \mathcal{L}_{a, \cdot} - \log(a)h - v\|^2 + \theta_1 Q(Dh, Dv; \theta_2)$$

Lin. reg.  $\hat{h}^{\text{LR}}$

$(\theta_1, \theta_2) = (0, 0)$



# Regularization parameters selection

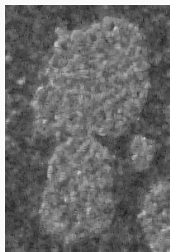
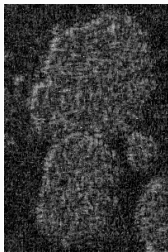
$$\left(\widehat{h}, \widehat{v}\right) (\mathcal{L}; \Theta) = \underset{h, v}{\operatorname{argmin}} \sum_a \|\log \mathcal{L}_{a, \cdot} - \log(a)h - v\|^2 + \theta_1 Q(Dh, Dv; \theta_2)$$

Lin. reg.  $\widehat{h}^{\text{LR}}$

Co-localized contours estimate  $\widehat{h}^{\text{C}}$

$(\theta_1, \theta_2) = (0, 0)$

$(\theta_1, \theta_2) = (0.5, 0.5)$



too small

# Regularization parameters selection

$$\left(\widehat{h}, \widehat{v}\right) (\mathcal{L}; \Theta) = \underset{h, v}{\operatorname{argmin}} \sum_a \left\| \log \mathcal{L}_{a, \cdot} - \log(a)h - v \right\|^2 + \theta_1 Q(Dh, Dv; \theta_2)$$

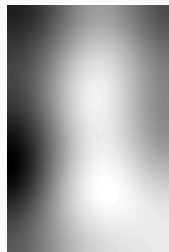
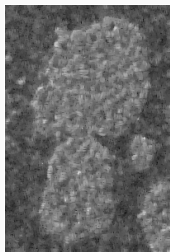
Lin. reg.  $\widehat{h}^{\text{LR}}$

Co-localized contours estimate  $\widehat{h}^{\text{C}}$

$(\theta_1, \theta_2) = (0, 0)$

$(\theta_1, \theta_2) = (0.5, 0.5)$

$(\theta_1, \theta_2) = (500, 500)$



too small

too large

# Regularization parameters selection

$$\left(\widehat{h}, \widehat{v}\right) (\mathcal{L}; \Theta) = \underset{h, v}{\operatorname{argmin}} \sum_a \|\log \mathcal{L}_{a, \cdot} - \log(a)h - v\|^2 + \theta_1 \mathcal{Q}(Dh, Dv; \theta_2)$$

Lin. reg.  $\widehat{h}^{\text{LR}}$

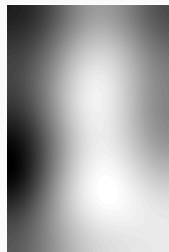
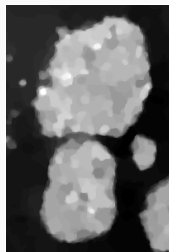
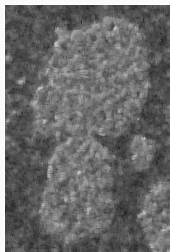
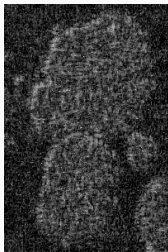
Co-localized contours estimate  $\widehat{h}^{\text{C}}$

$(\theta_1, \theta_2) = (0, 0)$

$(\theta_1, \theta_2) = (0.5, 0.5)$

$(\theta_1^\dagger, \theta_2^\dagger) = (11.5, 0.8)$

$(\theta_1, \theta_2) = (500, 500)$



too small

optimal

too large

What *optimal* means? How to determine  $\Theta^\dagger = (\theta_1^\dagger, \theta_2^\dagger)$ ?

## Parameter tuning (Grid search)

$$\left(\hat{\mathbf{h}}, \hat{\mathbf{v}}\right) (\mathcal{L}; \Theta) = \underset{\mathbf{h}, \mathbf{v}}{\operatorname{argmin}} \sum_a \|\log \mathcal{L}_{a,\cdot} - \log(a)\mathbf{h} - \mathbf{v}\|^2 + \theta_1 Q(D\mathbf{h}, D\mathbf{v}; \theta_2)$$

$\mathbf{h}$ : *discriminant*,  $\mathbf{v}$ : *auxiliary*

## Parameter tuning (Grid search)

$$\left(\hat{\mathbf{h}}, \hat{\mathbf{v}}\right) (\mathcal{L}; \Theta) = \underset{\mathbf{h}, \mathbf{v}}{\operatorname{argmin}} \sum_a \|\log \mathcal{L}_{a,\cdot} - \log(a)\mathbf{h} - \mathbf{v}\|^2 + \theta_1 \mathcal{Q}(\mathbf{D}\mathbf{h}, \mathbf{D}\mathbf{v}; \theta_2)$$

$\mathbf{h}$ : *discriminant*,  $\mathbf{v}$ : *auxiliary*

$\bar{\mathbf{h}}$ : *true regularity*

$$\mathcal{R}(\Theta) = \left\| \hat{\mathbf{h}}(\mathcal{L}; \Theta) - \bar{\mathbf{h}} \right\|^2$$

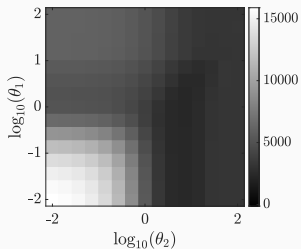
## Parameter tuning (Grid search)

$$\left(\hat{\mathbf{h}}, \hat{\mathbf{v}}\right)(\mathcal{L}; \Theta) = \underset{\mathbf{h}, \mathbf{v}}{\operatorname{argmin}} \sum_a \|\log \mathcal{L}_{a,\cdot} - \log(a)\mathbf{h} - \mathbf{v}\|^2 + \theta_1 Q(D\mathbf{h}, D\mathbf{v}; \theta_2)$$

$\mathbf{h}$ : discriminant,  $\mathbf{v}$ : auxiliary

$\bar{\mathbf{h}}$ : true regularity

$$\mathcal{R}(\Theta) = \left\| \hat{\mathbf{h}}(\mathcal{L}; \Theta) - \bar{\mathbf{h}} \right\|^2$$



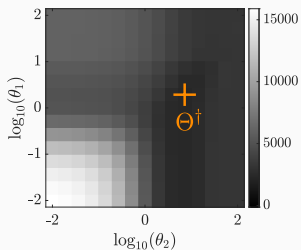
## Parameter tuning (Grid search)

$$(\hat{\mathbf{h}}, \hat{\mathbf{v}}) (\mathcal{L}; \Theta) = \underset{\mathbf{h}, \mathbf{v}}{\operatorname{argmin}} \sum_a \|\log \mathcal{L}_{a,\cdot} - \log(a)\mathbf{h} - \mathbf{v}\|^2 + \theta_1 Q(D\mathbf{h}, D\mathbf{v}; \theta_2)$$

$\mathbf{h}$ : discriminant,  $\mathbf{v}$ : auxiliary

$\bar{\mathbf{h}}$ : true regularity

$$\mathcal{R}(\Theta) = \|\hat{\mathbf{h}}(\mathcal{L}; \Theta) - \bar{\mathbf{h}}\|^2$$



## Parameter tuning (Grid search)

$$(\hat{h}, \hat{v}) (\mathcal{L}; \Theta) = \underset{h, v}{\operatorname{argmin}} \sum_a \|\log \mathcal{L}_{a, \cdot} - \log(a) \mathbf{h} - \mathbf{v}\|^2 + \theta_1 Q(D\mathbf{h}, D\mathbf{v}; \theta_2)$$

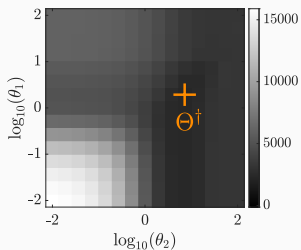
$\mathbf{h}$ : discriminant,  $\mathbf{v}$ : auxiliary

$\bar{h}$ : true regularity

$\bar{h}$ : unknown!

$$\mathcal{R}(\Theta) = \|\hat{h}(\mathcal{L}; \Theta) - \bar{h}\|^2$$

?



## Parameter tuning (Grid search)

$$(\hat{\mathbf{h}}, \hat{\mathbf{v}}) (\mathcal{L}; \Theta) = \underset{\mathbf{h}, \mathbf{v}}{\operatorname{argmin}} \sum_a \|\log \mathcal{L}_{a,\cdot} - \log(a)\mathbf{h} - \mathbf{v}\|^2 + \theta_1 \mathcal{Q}(\mathbf{D}\mathbf{h}, \mathbf{D}\mathbf{v}; \theta_2)$$

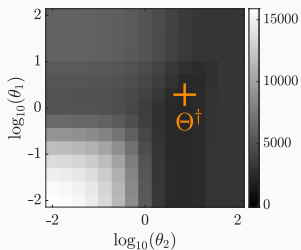
$\mathbf{h}$ : discriminant,  $\mathbf{v}$ : auxiliary

$\bar{\mathbf{h}}$ : true regularity

$$\mathcal{R}(\Theta) = \|\hat{\mathbf{h}}(\mathcal{L}; \Theta) - \bar{\mathbf{h}}\|^2$$

$\bar{\mathbf{h}}$ : unknown!

?



*Stein Unbiased Risk  
Estimate  
(SURE)*

## Stein Unbiased Risk Estimate (Principle)

Observations  $z = \bar{x} + \mathbf{n} \in \mathbb{R}^P$ ,  $\bar{x}$ : truth and  $\mathbf{n} \sim \mathcal{N}(0, \kappa^2 \mathbf{I}_P)$

## Stein Unbiased Risk Estimate (Principle)

**Observations**  $z = \bar{x} + \mathbf{n} \in \mathbb{R}^P$ ,  $\bar{x}$ : truth and  $\mathbf{n} \sim \mathcal{N}(0, \kappa^2 \mathbf{I}_P)$

**Parametric estimator**  $(z; \theta) \mapsto \hat{\mathbf{x}}(z; \theta)$

$$\mathbf{Ex.} \quad \hat{\mathbf{x}}(z; \theta) = \begin{cases} (\mathbf{I} + \theta \mathbf{D}^\top \mathbf{D})^{-1} z & \text{(linear)} \\ \underset{\mathbf{x}}{\operatorname{argmin}} \|z - \mathbf{x}\|^2 + \theta Q(\mathbf{D}\mathbf{x}) & \text{(nonlinear)} \end{cases}$$

## Stein Unbiased Risk Estimate (Principle)

**Observations**  $z = \bar{x} + \mathbf{n} \in \mathbb{R}^P$ ,  $\bar{x}$ : truth and  $\mathbf{n} \sim \mathcal{N}(0, \kappa^2 \mathbf{I}_P)$

**Parametric estimator**  $(z; \theta) \mapsto \hat{\mathbf{x}}(z; \theta)$

$$\text{Ex. } \hat{\mathbf{x}}(z; \theta) = \begin{cases} (\mathbf{I} + \theta \mathbf{D}^\top \mathbf{D})^{-1} z & \text{(linear)} \\ \underset{\mathbf{x}}{\operatorname{argmin}} \|z - \mathbf{x}\|^2 + \theta Q(\mathbf{D}\mathbf{x}) & \text{(nonlinear)} \end{cases}$$

**Quadratic error**  $R(\theta) \triangleq \mathbb{E}_{\mathbf{n}} \|\hat{\mathbf{x}}(z; \theta) - \bar{\mathbf{x}}\|^2 \stackrel{?}{=} \mathbb{E}_{\mathbf{n}} \hat{R}(z; \theta)$   $\bar{\mathbf{x}}$  unknown

# Stein Unbiased Risk Estimate (Principle)

**Observations**  $z = \bar{x} + \mathbf{n} \in \mathbb{R}^P$ ,  $\bar{x}$ : truth and  $\mathbf{n} \sim \mathcal{N}(0, \kappa^2 \mathbf{I}_P)$

**Parametric estimator**  $(z; \theta) \mapsto \hat{\mathbf{x}}(z; \theta)$

$$\text{Ex. } \hat{\mathbf{x}}(z; \theta) = \begin{cases} (\mathbf{I} + \theta \mathbf{D}^\top \mathbf{D})^{-1} z & \text{(linear)} \\ \underset{\mathbf{x}}{\operatorname{argmin}} \|z - \mathbf{x}\|^2 + \theta Q(\mathbf{D}\mathbf{x}) & \text{(nonlinear)} \end{cases}$$

**Quadratic error**  $R(\theta) \triangleq \mathbb{E}_{\mathbf{n}} \|\hat{\mathbf{x}}(z; \theta) - \bar{\mathbf{x}}\|^2 \stackrel{?}{=} \mathbb{E}_{\mathbf{n}} \hat{R}(z; \theta)$  ̄x unknown

**Theorem** [C. M. Stein, 1981, *Annals Stat.*]

Let  $(z; \theta) \mapsto \hat{\mathbf{x}}(z; \theta)$  an estimator of  $\bar{\mathbf{x}}$

- weakly differentiable w.r.t.  $z$ ,
- such that  $\mathbf{n} \mapsto \langle \hat{\mathbf{x}}(\bar{\mathbf{x}} + \mathbf{n}; \theta), \mathbf{n} \rangle$  is integrable w.r.t.  $\mathcal{N}(0, \kappa^2 \mathbf{I}_P)$ .


$$\begin{aligned} \hat{R}(z; \theta) &\triangleq \|\hat{\mathbf{x}}(z; \theta) - z\|^2 + 2\kappa^2 \operatorname{tr}(\partial_z \hat{\mathbf{x}}(z; \theta)) - \kappa^2 P \\ &\implies R(\theta) = \mathbb{E}_{\mathbf{n}}[\hat{R}(z; \theta)]. \end{aligned}$$

## Generalized *Stein Unbiased Risk Estimate*

**Observations**  $z = \mathbf{A}\bar{x} + \mathbf{n} \in \mathbb{R}^P$ ,  $\bar{x} \in \mathbb{R}^N$ ,  $\mathbf{A} : \mathbb{R}^{P \times N}$  and  $\mathbf{n} \sim \mathcal{N}(0, \mathcal{S})$

**E.g. the estimators**  $\hat{\mathbf{h}}(\mathcal{L}; \Theta)$  **with free or co-localized contours**

$$\log \mathcal{L} = \mathbf{A}(\bar{\mathbf{h}}, \bar{\mathbf{v}}) + \mathbf{n} \quad \mathbf{n} \sim \mathcal{N}(0, \mathcal{S}) \quad \mathcal{R} = \|\hat{\mathbf{h}} - \bar{\mathbf{h}}\|^2$$

$$\mathbf{A} : (\mathbf{h}, \mathbf{v}) \mapsto \{\log(a)\mathbf{h} + \mathbf{v}\}_a \quad \Pi : (\mathbf{h}, \mathbf{v}) \mapsto (\mathbf{h}, 0)$$



**Projected estimation error**  $R_{\Pi}(\Theta) \triangleq \mathbb{E}_{\mathbf{n}} \|\Pi \hat{\mathbf{x}}(z; \Theta) - \Pi \bar{\mathbf{x}}\|^2$

# Generalized Stein Unbiased Risk Estimate

**Observations**  $z = \mathbf{A}\bar{x} + \mathbf{n} \in \mathbb{R}^P$ ,  $\bar{x} \in \mathbb{R}^N$ ,  $\mathbf{A} : \mathbb{R}^{P \times N}$  and  $\mathbf{n} \sim \mathcal{N}(0, \mathcal{S})$

**E.g. the estimators**  $\hat{h}(\mathcal{L}; \Theta)$  **with free or co-localized contours**

$$\log \mathcal{L} = \mathbf{A}(\bar{h}, \bar{v}) + \mathbf{n} \quad \mathbf{n} \sim \mathcal{N}(0, \mathcal{S}) \quad \mathcal{R} = \|\hat{h} - \bar{h}\|^2$$

$$\mathbf{A} : (h, v) \mapsto \{\log(a)h + v\}_a \quad \Pi : (h, v) \mapsto (h, 0)$$


**Projected estimation error**  $R_{\Pi}(\Theta) \triangleq \mathbb{E}_{\mathbf{n}} \|\Pi \hat{x}(z; \Theta) - \Pi \bar{x}\|^2$

**Theorem** (B. Pascal et al., 2020, *J. Math. Imaging Vis.*)

Let  $(z; \Theta) \mapsto \hat{x}(z; \Theta)$  an estimator of  $\bar{x}$

- weakly differentiable w.r.t.  $z$ ,
- such that  $\mathbf{n} \mapsto \langle \Pi \hat{x}(\bar{x} + \mathbf{n}; \Theta), \Phi \mathbf{n} \rangle$  is integrable w.r.t.  $\mathcal{N}(0, \mathcal{S})$ .

$$\hat{R}(\Theta) \triangleq \|\Phi(\mathbf{A}\hat{x}(z; \Theta) - z)\|^2 + 2\text{tr}(\mathcal{S}\Phi^{\top}\Pi\partial_z\hat{x}(z; \Theta)) - \text{tr}(\Phi\mathcal{S}\Phi^{\top})$$

$$\implies R_{\Pi}(\Theta) = \mathbb{E}_{\mathbf{n}}[\hat{R}(\Theta)].$$

## Computation of the degrees of freedom

Degrees of freedom

$$\text{dof} \triangleq \text{tr} (\mathcal{S}\Phi^\top \Pi \partial_z \hat{x}(z; \Theta))$$

# Computation of the degrees of freedom

Degrees of freedom  $\text{dof} \triangleq \text{tr}(\mathcal{S}\Phi^\top \Pi \partial_z \hat{x}(z; \Theta))$

- **Monte Carlo strategy (MC)**      **Large size matrix**  $M \in \mathbb{R}^{P \times P}$

$$\text{tr}(M) = \mathbb{E}_\varepsilon \langle M\varepsilon, \varepsilon \rangle, \quad \varepsilon \sim \mathcal{N}(0, I_P)$$

# Computation of the degrees of freedom

Degrees of freedom  $\text{dof} \triangleq \text{tr}(\mathcal{S}\Phi^\top \Pi \partial_z \hat{x}(z; \Theta))$

- **Monte Carlo strategy (MC)** **Large size matrix**  $M \in \mathbb{R}^{P \times P}$

$$\text{tr}(M) = \mathbb{E}_\varepsilon \langle M\varepsilon, \varepsilon \rangle, \quad \varepsilon \sim \mathcal{N}(0, I_P)$$

- **Finite Differences (FD)** **Inaccessible Jacobian matrix**

$$\partial_z \hat{x}[\varepsilon] \underset{\nu \rightarrow 0}{\simeq} \frac{1}{\nu} (\hat{x}(z + \nu\varepsilon; \Theta) - \hat{x}(z; \Theta))$$

# Computation of the degrees of freedom

Degrees of freedom  $\text{dof} \triangleq \text{tr}(\mathcal{S}\Phi^\top \Pi \partial_z \hat{x}(z; \Theta))$

- **Monte Carlo strategy (MC)** **Large size matrix**  $M \in \mathbb{R}^{P \times P}$

$$\text{tr}(M) = \mathbb{E}_\varepsilon \langle M\varepsilon, \varepsilon \rangle, \quad \varepsilon \sim \mathcal{N}(0, I_P)$$

- **Finite Differences (FD)** **Inaccessible Jacobian matrix**

$$\partial_z \hat{x}[\varepsilon] \underset{\nu \rightarrow 0}{\simeq} \frac{1}{\nu} (\hat{x}(z + \nu\varepsilon; \Theta) - \hat{x}(z; \Theta))$$

**Proposition** (B. Pascal et al., 2020, *J. Math. Imaging Vis.*)

Let  $(z; \Theta) \mapsto \hat{x}(z; \Theta)$  an estimator of  $\bar{x}$

- uniformly Lipschitz continuous w.r.t.  $z$ ,
- such that  $\forall \Theta \in \mathbb{R}^T$ ,  $\hat{x}(0_P; \Theta) = 0_N$ . Then

$$\mathbb{E}_n[\text{dof}] = \lim_{\nu \rightarrow 0} \mathbb{E}_{n,\varepsilon} \left[ \frac{1}{\nu} \langle \mathcal{S}\Phi^\top \Pi (\hat{x}(z + \nu\varepsilon; \Theta) - \hat{x}(z; \Theta)), \varepsilon \rangle \right]$$

## Estimation of the covariance structure of leader coefficients

**Log-Gaussianity:**  $\log \mathcal{L} = A(\bar{\mathbf{h}}, \bar{\mathbf{v}}) + \mathbf{n}$  with  $\mathbf{n} \sim \mathcal{N}(0, \mathcal{S})$

$\implies$  Necessary to provide some estimate  $\hat{\mathcal{S}}$  to compute dof and then  $\hat{R}$

# Estimation of the covariance structure of leader coefficients

**Log-Gaussianity:**  $\log \mathcal{L} = A(\bar{\mathbf{h}}, \bar{\mathbf{v}}) + \mathbf{n}$  with  $\mathbf{n} \sim \mathcal{N}(0, \mathcal{S})$

$\implies$  Necessary to provide some estimate  $\hat{\mathcal{S}}$  to compute dof and then  $\hat{R}$

**Covariance structure** Noise  $\zeta_{j, \underline{n}}$  on  $\log \mathcal{L}_{j, \underline{n}}$  at scale  $2^j$  and pixel  $\underline{n} = (n_1, n_2)$

$$\mathcal{S}_{j, \underline{n}}^{j', \underline{n}'} \triangleq \mathbb{E} \zeta_{j, \underline{n}} \zeta_{j', \underline{n}'} = \mathcal{C}_j^{j'} \Xi_j^{j'}(\underline{n} - \underline{n}'), \quad \text{where } \mathcal{C}_j^{j'} \triangleq \mathbb{E} \zeta_{j, \underline{n}} \zeta_{j', \underline{n}}$$

- $\mathcal{C}_j^{j'}$  independent of  $\underline{n}$ : inter-scale covariance
- $\Xi_j^{j'}$ : stationary spatial correlations, with correlation length  $\max(2^j, 2^{j'})$

# Estimation of the covariance structure of leader coefficients

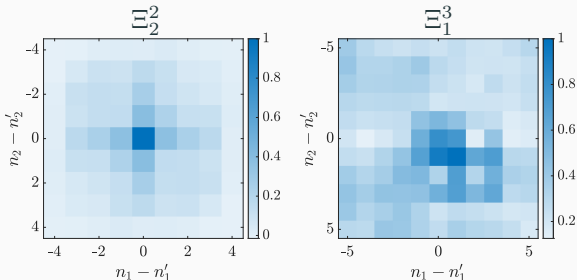
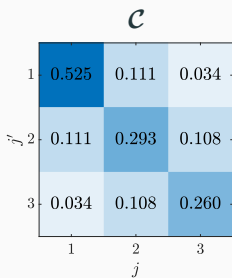
**Log-Gaussianity:**  $\log \mathcal{L} = A(\bar{\mathbf{h}}, \bar{\mathbf{v}}) + \mathbf{n}$  with  $\mathbf{n} \sim \mathcal{N}(0, \mathcal{S})$

$\implies$  Necessary to provide some estimate  $\hat{\mathcal{S}}$  to compute dof and then  $\hat{R}$

**Covariance structure** Noise  $\zeta_{j,\underline{n}}$  on  $\log \mathcal{L}_{j,\underline{n}}$  at scale  $2^j$  and pixel  $\underline{n} = (n_1, n_2)$

$$\mathcal{S}_{j,\underline{n}}^{j',\underline{n}'} \triangleq \mathbb{E} \zeta_{j,\underline{n}} \zeta_{j',\underline{n}'} = \mathcal{C}_j^{j'} \Xi_j^{j'}(\underline{n} - \underline{n}'), \quad \text{where } \mathcal{C}_j^{j'} \triangleq \mathbb{E} \zeta_{j,\underline{n}} \zeta_{j',\underline{n}}$$

- $\mathcal{C}_j^{j'}$  independent of  $\underline{n}$ : inter-scale covariance
- $\Xi_j^{j'}$ : stationary spatial correlations, with correlation length  $\max(2^j, 2^{j'})$



## Parameter tuning (Grid search)

$$(\hat{h}, \hat{v}) (\mathcal{L}; \Theta) = \underset{h, v}{\operatorname{argmin}} \sum_a \|\log \mathcal{L}_{a, \cdot} - \log(a)h - v\|^2 + \theta_1 \mathcal{Q}(\text{D}h, \text{D}v; \theta_2)$$

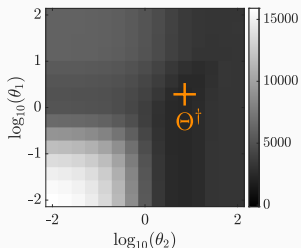
$h$ : discriminant,  $v$ : auxiliary

$\bar{h}$ : true regularity

$\bar{h}$ : unknown!

$$\mathcal{R}(\Theta) = \left\| \hat{h}(\mathcal{L}; \Theta) - \bar{h} \right\|^2$$

$$\hat{R}_{\nu, \varepsilon}(\mathcal{L}; \Theta | \mathcal{S})$$



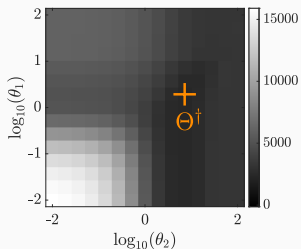
# Parameter tuning (Grid search)

$$(\hat{h}, \hat{v}) (\mathcal{L}; \Theta) = \underset{h, v}{\operatorname{argmin}} \sum_a \|\log \mathcal{L}_{a, \cdot} - \log(a)h - v\|^2 + \theta_1 \mathcal{Q}(\operatorname{Dh}, \operatorname{Dv}; \theta_2)$$

$h$ : discriminant,  $v$ : auxiliary

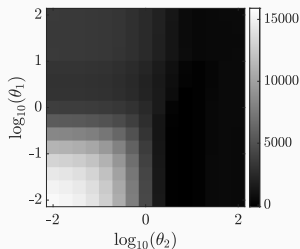
$\bar{h}$ : true regularity

$$\mathcal{R}(\Theta) = \left\| \hat{h}(\mathcal{L}; \Theta) - \bar{h} \right\|^2$$



$\bar{h}$ : unknown!

$$\hat{R}_{\nu, \varepsilon}(\mathcal{L}; \Theta | \mathcal{S})$$



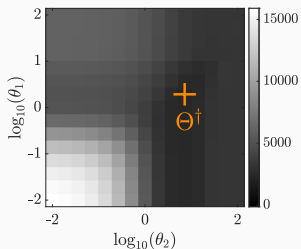
## Parameter tuning (Grid search)

$$\left(\widehat{h}, \widehat{v}\right) (\mathcal{L}; \Theta) = \underset{h, v}{\operatorname{argmin}} \sum_a \|\log \mathcal{L}_{a, \cdot} - \log(a)h - v\|^2 + \theta_1 \mathcal{Q}(\operatorname{Dh}, \operatorname{Dv}; \theta_2)$$

$h$ : discriminant,  $v$ : auxiliary

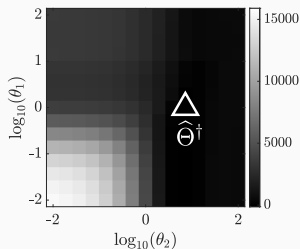
$\bar{h}$ : true regularity

$$\mathcal{R}(\Theta) = \left\| \widehat{h}(\mathcal{L}; \Theta) - \bar{h} \right\|^2$$



$\bar{h}$ : unknown!

$$\widehat{R}_{\nu, \varepsilon}(\mathcal{L}; \Theta | \mathcal{S})$$



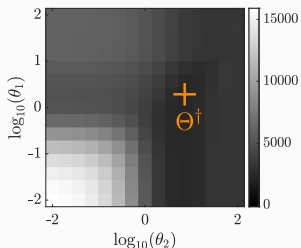
## Parameter tuning (Grid search)

$$(\hat{h}, \hat{v}) (\mathcal{L}; \Theta) = \underset{h, v}{\operatorname{argmin}} \sum_a \|\log \mathcal{L}_{a, \cdot} - \log(a)h - v\|^2 + \theta_1 \mathcal{Q}(\operatorname{Dh}, \operatorname{Dv}; \theta_2)$$

$h$ : discriminant,  $v$ : auxiliary

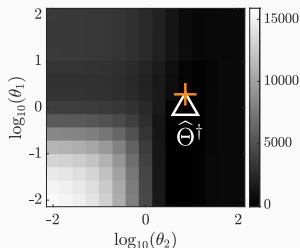
$\bar{h}$ : true regularity

$$\mathcal{R}(\Theta) = \|\hat{h}(\mathcal{L}; \Theta) - \bar{h}\|^2$$



$\bar{h}$ : unknown!

$$\hat{R}_{\nu, \varepsilon}(\mathcal{L}; \Theta | \mathcal{S})$$



# Parameter tuning (Automatic selection)

$$(\hat{h}, \hat{v}) (\mathcal{L}; \Theta) = \underset{h, v}{\operatorname{argmin}} \sum_a \|\log \mathcal{L}_{a, \cdot} - \log(a)h - v\|^2 + \theta_1 \mathcal{Q}(\text{Dh}, \text{Dv}; \theta_2)$$

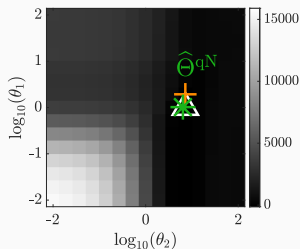
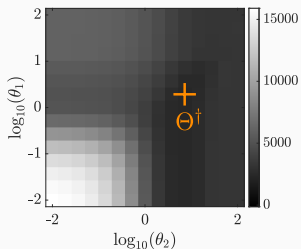
$h$ : discriminant,  $v$ : auxiliary

$\bar{h}$ : true regularity

$$\mathcal{R}(\Theta) = \|\hat{h}(\mathcal{L}; \Theta) - \bar{h}\|^2$$

$\bar{h}$ : unknown!

$$\hat{R}_{\nu, \varepsilon}(\mathcal{L}; \Theta | \mathcal{S})$$



# Parameter tuning (Automatic selection)

$$(\hat{h}, \hat{v}) (\mathcal{L}; \Theta) = \underset{h, v}{\operatorname{argmin}} \sum_a \|\log \mathcal{L}_{a, \cdot} - \log(a)h - v\|^2 + \theta_1 \mathcal{Q}(\operatorname{Dh}, \operatorname{Dv}; \theta_2)$$

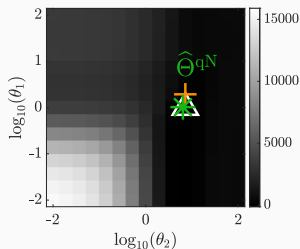
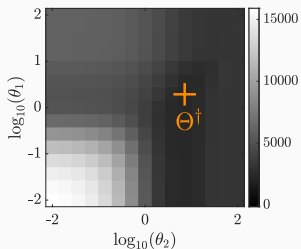
$h$ : discriminant,  $v$ : auxiliary

$\bar{h}$ : true regularity

$$\mathcal{R}(\Theta) = \|\hat{h}(\mathcal{L}; \Theta) - \bar{h}\|^2$$

$\bar{h}$ : unknown!

$$\hat{R}_{\nu, \varepsilon}(\mathcal{L}; \Theta | \mathcal{S})$$



# Automated selection of regularization parameters

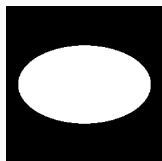
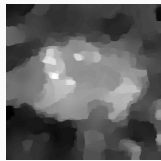
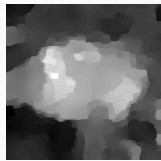
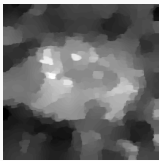
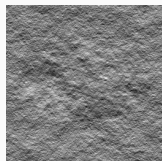
$$(\hat{h}, \hat{v}) (\mathcal{L}; \Theta) = \operatorname{argmin}_{h, v} \sum_a \|\log \mathcal{L}_{a, \cdot} - \log(a)h - v\|^2 + \theta_1 Q(Dh, Dv; \theta_2)$$

**Example**

$\hat{h}^F(\mathcal{L}; \Theta^\dagger)$   
(grid)

$\hat{h}^F(\mathcal{L}; \hat{\Theta}^\dagger)$   
(grid)

$\hat{h}^F(\mathcal{L}; \hat{\Theta}^{qN})$   
(quasi-Newton)



**225** calls of the estimator over the grid v.s. **40** for quasi-Newton

# Isotropic texture segmentation: take home messages

- ▶ **Fractal texture model based on local *regularity* and *variance***
  - appropriate for real-world texture characterization
  - complementary attributes able to finely discriminate

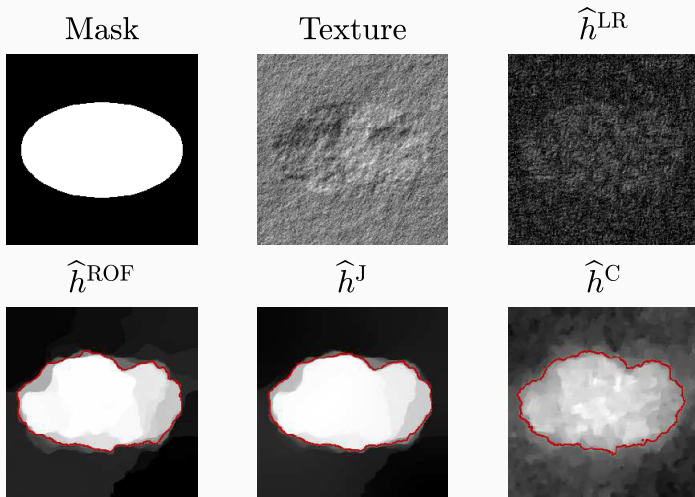
# Isotropic texture segmentation: take home messages

- ▶ **Fractal texture model based on local *regularity* and *variance***
  - appropriate for real-world texture characterization
  - complementary attributes able to finely discriminate
  
- ▶ **Simultaneous estimation and regularization**
  - significant decrease of the estimation error
  - accurate and regular *co-localized* contours

# Isotropic texture segmentation: take home messages

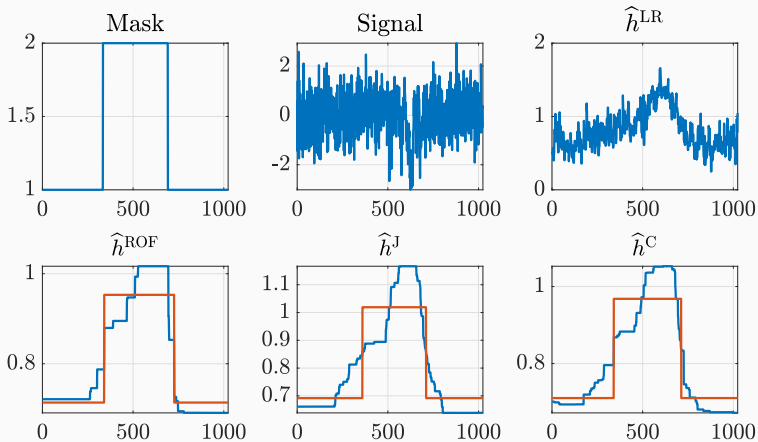
- ▶ **Fractal texture model based on local *regularity* and *variance***
  - appropriate for real-world texture characterization
  - complementary attributes able to finely discriminate
- ▶ **Simultaneous estimation and regularization**
  - significant decrease of the estimation error
  - accurate and regular *co-localized* contours
- ▶ **Fast algorithms for automated tuning of hyperparameters**
  - possibility to manage huge amount of data
  - amenable to process data corrupted by *correlated* noise
  - ensured objectivity and reproducibility

# GSUGAR: Matlab toolbox for texture segmentation



[github.com/bpascal-fr/gsugar](https://github.com/bpascal-fr/gsugar): demo\_gsugar\_2D

# GSUGAR: Changepoint detection in monofractal signals



[github.com/bpascal-fr/g sugar](https://github.com/bpascal-fr/g sugar): demo\_gsugar\_1D

# **Anisotropic textures analysis**

---

# Anisotropic fractal textures in real data

## Breast cancer:

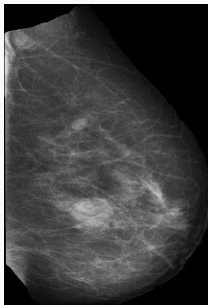
- most common cancer amongst women with  $\sim 1$  over 8 diagnosed
- early detection is critical for the patient's survival

# Anisotropic fractal textures in real data

## Breast cancer:

- most common cancer amongst women with  $\sim 1$  over 8 diagnosed
- early detection is critical for the patient's survival

**X-ray imaging:** most used imaging technique yielding a so-called *mammogram*

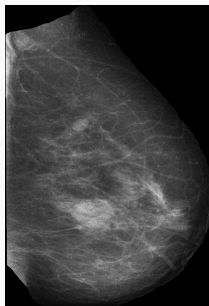


# Anisotropic fractal textures in real data

## Breast cancer:

- most common cancer amongst women with  $\sim 1$  over 8 diagnosed
- early detection is critical for the patient's survival

**X-ray imaging:** most used imaging technique yielding a so-called *mammogram*



## Assessment by a radiologist:

- fatty tissues: translucent to X-rays (black)
- epithelial & stromal tissues: absorb X-rays (white)
- tumorous tissues: **also absorb X-rays** (white)

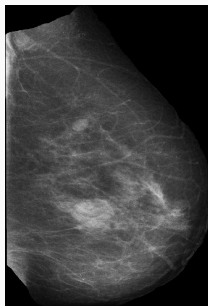
⇒ errors of both I and II types in anomaly detection

# Anisotropic fractal textures in real data

## Breast cancer:

- most common cancer amongst women with  $\sim 1$  over 8 diagnosed
- early detection is critical for the patient's survival

**X-ray imaging:** most used imaging technique yielding a so-called *mammogram*



## Assessment by a radiologist:

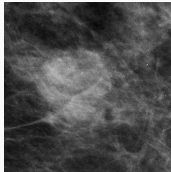
- fatty tissues: translucent to X-rays (black)
- epithelial & stromal tissues: absorb X-rays (white)
- tumorous tissues: **also absorb X-rays** (white)

⇒ errors of both I and II types in anomaly detection

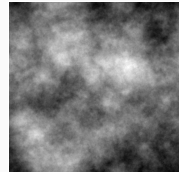
**Computer-Aided Detection:** used in 92% of screening mammograms in U.S.

# Anisotropic fractal textures in real data

Self-similar textures:



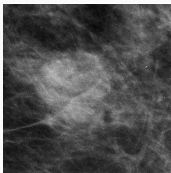
Mammogram



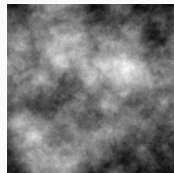
fractional Brownian field

# Anisotropic fractal textures in real data

Self-similar textures:



Mammogram



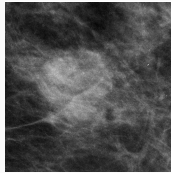
fractional Brownian field

**Isotropic fractal analysis**, e.g., fractal dimension of a rough surface, for

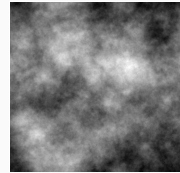
- classification of mammogram density [Caldwell et al., 1990, *Phys. Med. Biol.*]
- lesion detection in mammograms [Burgess et al., 2001, *Med. Biol.*]
- assessment of breast cancer risk [Heine et al., 2002, *Acad. Radiol.*]

# Anisotropic fractal textures in real data

Self-similar textures:



Mammogram

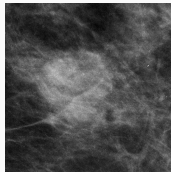


fractional Brownian field

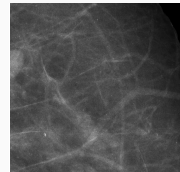
**Isotropic fractal analysis**, e.g., fractal dimension of a rough surface, for

- classification of mammogram density [Caldwell et al., 1990, *Phys. Med. Biol.*]
- lesion detection in mammograms [Burgess et al., 2001, *Med. Biol.*]
- assessment of breast cancer risk [Heine et al., 2002, *Acad. Radiol.*]

**Anisotropy in mammograms**



mass



tissues

## Anisotropic Self-Similar Fields

**Definition:** Let  $f \in L^1(\min(1, |\underline{\xi}|^2)d\underline{\xi})$  a **spectral density**. The associated *Bonami-Estrade field*  $X^f$  is defined through its harmonizable representation:

$$X^f : \begin{cases} \mathbb{R}^2 & \rightarrow & \mathbb{R} \\ \underline{x} & \mapsto & \int_{\mathbb{R}^2} (\exp(i\underline{x} \cdot \underline{\xi}) - 1) \sqrt{f(\underline{\xi})} \tilde{W}(d\underline{\xi}) \end{cases}$$

with  $W$  a Brownian measure;  $\tilde{W}$  its Fourier transform.

[A. Bonami & A. Estrade, 2003, *J. Fourier Anal. Appl.*]

# Anisotropic Self-Similar Fields

**Definition:** Let  $f \in L^1(\min(1, |\underline{\xi}|^2)d\underline{\xi})$  a **spectral density**. The associated *Bonami-Estrade field*  $X^f$  is defined through its harmonizable representation:

$$X^f : \begin{cases} \mathbb{R}^2 & \rightarrow & \mathbb{R} \\ \underline{x} & \mapsto & \int_{\mathbb{R}^2} (\exp(i\underline{x} \cdot \underline{\xi}) - 1) \sqrt{f(\underline{\xi})} \tilde{W}(d\underline{\xi}) \end{cases}$$

with  $W$  a Brownian measure;  $\tilde{W}$  its Fourier transform.

[A. Bonami & A. Estrade, 2003, *J. Fourier Anal. Appl.*]

**Spectral density** encodes visual and statistical properties such as

- (an)isotropy
- preferential directions
- short or long range dependencies

[H. Biermé, 2019, *Lecture Notes in Mathematics*, Springer]

# The Anisotropic Fractional Brownian Field

The **anisotropic fractional Brownian field** is defined as

$$X^f(\underline{x}) = \int_{\mathbb{R}^2} (\exp(i\underline{x} \cdot \underline{\xi}) - 1) \sqrt{f(\underline{\xi})} \tilde{W}(d\underline{\xi})$$

with **spectral density**  $f(\underline{\xi}) = \tau\left(\frac{\underline{\xi}}{\|\underline{\xi}\|}\right) \|\underline{\xi}\|^{-2h} \left(\frac{\underline{\xi}}{\|\underline{\xi}\|}\right)^{-2}$  with

- $\tau : \mathbb{S}_1 \rightarrow \mathbb{R}_+$  the **topothesy** function
- $h : \mathbb{S}_1 \rightarrow ]0, 1[$  the **Hurst** function

Package PyAFBF for the simulation of rough anisotropic image textures

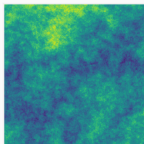
[fjprichard.github.io/PyAFBF](https://github.com/fjprichard/PyAFBF)

[F. J. Richard & H. Biermé, 2011, *J. Math. Imaging Vis.*]

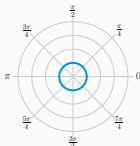
# Particular (anisotropic) fractional Brownian fields

**$H$ -fractional Brownian field  $H$ -fBf:**  $h \equiv H$ ,  $\tau \equiv \sigma^2/C_H$  both **constant**

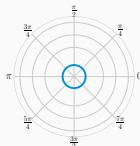
Field  $X^f$



Hurst function  $h$



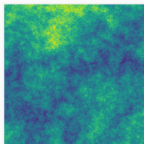
Topothesy function  $\tau$



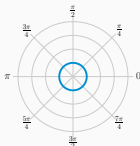
# Particular (anisotropic) fractional Brownian fields

**$H$ -fractional Brownian field  $H$ -fBf:**  $h \equiv H$ ,  $\tau \equiv \sigma^2/C_H$  both **constant**

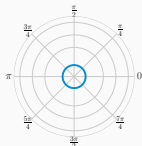
Field  $X^f$



Hurst function  $h$



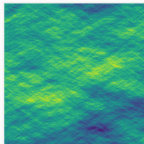
Topothesis function  $\tau$



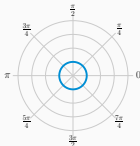
**$H$ -anisotropic fractional Brownian field  $H$ -afBf:**  $h \equiv H$  **constant**

$\implies$  directional modulation of the variance of the field via  $\tau$

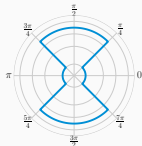
Field  $X^f$



Hurst function  $h$



Topothesis function  $\tau$



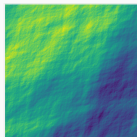
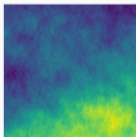
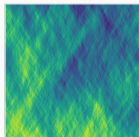
# General anisotropic fractional Brownian fields

**Anisotropic fractional Brownian field afBf:** modulation of both

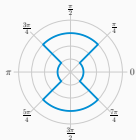
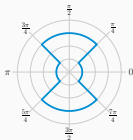
⇒ the variance of the field via  $\tau$

⇒ the decay the spectral density via  $h$

$\chi^f$



$h(\vartheta)$



$\tau(\vartheta)$



# Uniform Hölder regularity of anisotropic fields

**Definition:** The uniform Hölder regularity of the field  $X^f$  is  $H_{\min}$  if

$$\exists A, B > 0, \quad \text{such that: } \forall \|\underline{\xi}\| > A, \quad f(\underline{\xi}) \leq B \|\underline{\xi}\|^{-2H_{\min}-2}.$$

**Anisotropic fractional Brownian fields** have uniform Hölder regularity

$$H_{\min} = \operatorname{ess\,inf}_{\vartheta \in \mathbb{S}_1} h(\vartheta)$$

From **Kolmogorov-Chensov theorem**

- $H$ -(isotropic) fractional Brownian field  $B_H$ :  $H_{\min} = H$
- $H$ -anisotropic fractional Brownian field  $B_H$ :  $H_{\min} = H$

**Same** uniform Hölder regularity  $H_{\min}$  for  $H$ -fBf and  $H$ -afBf.

[S. Cohen & J. Istas, 2013, *Springer*]

# Analysis of anisotropic fractal textures

- **Directional increments & Radon transform:** [H. Biermé et al., 2008, *ESAIM: Proba. Stat.*]

$$(\forall(\vartheta, t) \in \mathbb{S}^1 \times \mathbb{R}) \quad \mathcal{R}_\rho X(\vartheta, t) = \int_{\mathbb{R}} X(s\vartheta^\perp + t\vartheta)\rho(s) ds$$

windowed Radon transform with  $\rho$  Schwartz class

# Analysis of anisotropic fractal textures

- **Directional increments & Radon transform:** [H. Biermé et al., 2008, *ESAIM: Proba. Stat.*]

$$(\forall(\vartheta, t) \in \mathbb{S}^1 \times \mathbb{R}) \quad \mathcal{R}_\rho X(\vartheta, t) = \int_{\mathbb{R}} X(s\vartheta^\perp + t\vartheta)\rho(s) ds$$

windowed Radon transform with  $\rho$  Schwartz class

- **X-let and scattering transform:** [S. Mallat, 2008, *Acad. Press*; J. Bruna, 2013, *PhD thesis*] [kymat.io](http://kymat.io)

scattering coefficients of order  $n$ :  $|||X * \psi_{\theta_1, j_1} | * \psi_{\theta_2, j_2} | \dots * \psi_{\theta_n, j_n} | * \varphi_J$

# Analysis of anisotropic fractal textures

- **Directional increments & Radon transform:** [H. Biermé et al., 2008, *ESAIM: Proba. Stat.*]

$$(\forall(\vartheta, t) \in \mathbb{S}^1 \times \mathbb{R}) \quad \mathcal{R}_\rho X(\vartheta, t) = \int_{\mathbb{R}} X(s\vartheta^\perp + t\vartheta)\rho(s) ds$$

windowed Radon transform with  $\rho$  Schwartz class

- **X-let and scattering transform:** [S. Mallat, 2008, *Acad. Press*; J. Bruna, 2013, *PhD thesis*] [kymat.io](http://kymat.io)

scattering coefficients of order  $n$ :  $|||X * \psi_{\theta_1, j_1} | * \psi_{\theta_2, j_2} | \dots * \psi_{\theta_n, j_n} | * \varphi_J$

- **Monogenic Images** [H. Biermé et al., 2024, *Preprint*]

$$\mathcal{M}X(\mathbf{w}) = (\langle X, \mathbf{w} \rangle, \langle \mathcal{R}_1 X, \mathbf{w} \rangle, \langle \mathcal{R}_2 X, \mathbf{w} \rangle)$$

$$\mathcal{R}_k \mathbf{w}(\underline{x}) = \frac{1}{2\pi} \lim_{\varepsilon \rightarrow 0} \int_{\mathbb{R}^2 \setminus B(0, \varepsilon)} \frac{x_k - y_k}{\|\underline{x} - \underline{y}\|^3} \mathbf{w}(\underline{y}) d\underline{y} \quad \text{Riesz transform}$$

# Wavelet analysis of anisotropic fractal textures

## Multiband complex wavelet transform

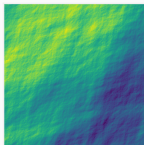
$(\psi^{(1)}, \dots, \psi^{(B)})$   $B$  complex mother wavelets:  $\psi^{(b)} : \mathbb{R}^2 \rightarrow \mathbb{C}$  such that

$$\psi^{(b)} = \psi^{(0)} (\mathcal{R}_{\vartheta_b}^\top \cdot) \quad \tilde{\psi}^{(b)} = \tilde{\psi}^{(0)} (\mathcal{R}_{\vartheta_b}^\top \cdot)$$

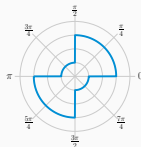
for  $\psi^{(0)}$  a frequency-direction selective complex mother wavelet;

**multiband wavelet coefficients:**  $\zeta_{j,\underline{k}}^{(b)} = \langle X, \psi_{j,\underline{k}}^{(b)} \rangle$

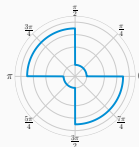
Field  $X^f$



Hurst function  $h$

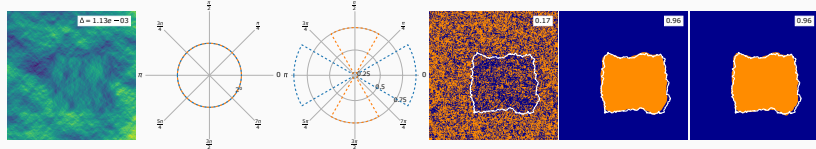


Topothesy function  $\tau$



# Segmentation of piecewise homogeneous anisotropic textures

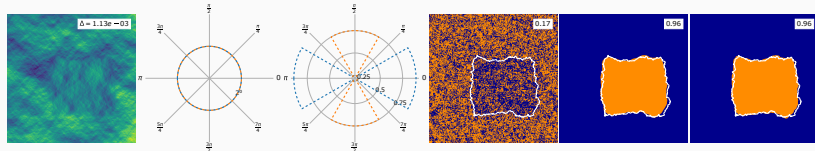
## Synthesis $M$ -class piecewise homogeneous Gaussian Bonami-Estrade field



- $M = 2$  textures: background vs. central rectangle
- **same** topothesy
- **different** Hurst functions

# Segmentation of piecewise homogeneous anisotropic textures

## Synthesis $M$ -class piecewise homogeneous Gaussian Bonami-Estrade field



- $M = 2$  textures: background vs. central rectangle
- same topology
- different Hurst functions

**Segmentation:** requires accurate contour localization

**Non-decimated Dual Tree Complex Wavelet Transform**  $\zeta_{j,\underline{n}}^{(b)}$

**Theorem** Let  $X^f$  a piecewise homogeneous Gaussian Bonami-Estrade field.

The multiband wavelet coefficients  $\zeta_{j,\underline{n}}^{(b)} = \langle X^f, \psi_{j,\underline{n}}^{(b)} \rangle$  satisfy

$$\zeta_{j,\underline{n}}^{(b)} \sim \mathcal{N}\left(0, \left(\sigma_{j,\underline{n}}^{(b)}\right)^2\right) \quad \text{with} \quad \left(\sigma_{j,\underline{n}}^{(b)}\right)^2 \sim \mathcal{V}(\tau, h, \psi^{(b)}) 2^{j2H(h, \psi^{(b)})}$$

## ▶ Non-decimated multiband wavelet coefficients

- behaves locally approximately as **power laws**
- local scaling exponents depending on **Hurst function**
- local intercept providing information about **topothesy function**

# Anisotropic texture segmentation: take home messages

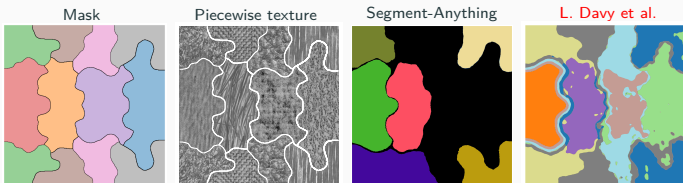
## ► Non-decimated multiband wavelet coefficients

- behaves locally approximately as **power laws**
- local scaling exponents depending on **Hurst function**
- local intercept providing information about **topothesy function**

## ► Regularized estimates of scaling exponents and intercept

- approximate **power-law** model for multiband wavelet coefficients
- penalization enforcing pixel-wise spatial **piecewise constancy**
- excellent segmentation performance in **various configurations**

## Natural textures characterized by joint fractal and anisotropy properties



[L. Davy et al., 2023, *ICASSP*; L. Davy et al., 2024, *EUSIPCO*;

L. Davy et al., 2025, *Preprint*]